VILLANOVA
UNIVERSITY

OFFICE OF THE DIRECTOR
CENTER FOR ADVANCED COMMUNICATIONS

July 19, 2018

John Tague, Ph.D.
ONR Ocean Sensing & Systems Apps Div
Code 321
Office of Naval Research
875 North Randolph Street
Arlington, VA 22203-1995

Dear Dr. Tague,

Enclosed, please find a copy of the Final Report for the ONR Grant no N00014-17-1-2396, tilted "Co-Prime Frequency and Aperture Design for HF Surveillance, Wideband Radar Imaging, and Nonstationary Array Processing," which ended June 30, 2018. I hope you find this report satisfactory.

Thank you,

Moeness Amin, PhD
Director, Center for Advanced Communications
Professor, Electrical & Computer Engineering

800 Lancaster Avenue | Villanova, Pennsylvania 19085 | PHONE 610 519-4263 | FAX 610 519-6118 | vil.anova.edu

College of ENGINEERING
VILLANOVA UNIVERSITY

CAC
Center for Advanced Communications
College of Engineering, Villanova University

FINAL TECHNICAL REPORT

(04/01/2017 - 06/30/2018)

Co-Prime Frequency and Aperture Design for HF Surveillance, Wideband Radar Imaging, and Nonstationary Array Processing

Submitted to

Office of Naval Research

ONR Grant: N00014-17-1-2396

Principal Investigator

Moeness Amin

Contributor

Prof. Moeness Amin

Mr. Ali Hamza

Table of Contents

1. Executive Summary

This report presents the results of the research performed under Office of Naval Research (ONR) grant number N00014-13-1-0061 over the period of April 1st, 2017 to June 30th, 2018. The research team working on this project consists of Prof. Moeness Amin (PI, Villanova University), Mr. Ali Hamza (PhD student, Villanova University), Dr. Joe Fabrizio (DSTG, Australia), Dr. Anastasios Deligiannis (Loughborough University, UK), and Dr. Sangarapillai Lambotharan(Loughborough University, UK).

The overaching research objectives are to develop novel co-prime sampling and array design strategies that achieve high-resolution estimation of spectral power distributions and signal direction-of-arrivals (DOAs), and their applications in various surveillance, radar imaging applications, and array processing. The focus of our studies has been in the following two areas: (i) Hybrid Sparse Array Beamforming Design for General Rank Signal Models Generalized co-prime array design; (ii) Optimum Sparse Subarray Design for Multitask Receivers.

The research efforts under this project haave resulted in four conference papers and two journal papers, one under review and the other completed it first revision. Below is a summary of the research accomplishments in each of the above two individual areas. A list of the publications generated under the support of this project is provided in Section 2. The contributions in the two journal paper are fully discussed and explained in Section 3. The summaries of these papers are as follows.

1.1 Hybrid Sparse Array Beamforming Design for General Rank Signal Models

The report considers sparse array design for receive beamforming achieving maximum signal-to-interference plus noise ratio (MaxSINR) for both single point source and multiple point sources, operating in an interference active environment. Unlike existing sparse design methods which either deal with structured environment-independent or non-structured environment-dependent arrays, our method is a hybrid approach and seeks a full augumentable array that optimizes beamformer performance. This approach proves important for limited aperture which constrains the number of possible uniform grid points for sensor placements. The problem is formulated as quadratically constraint quadratic program (QCQP), with the cost function penalized with weighted l_1-norm squared of the beamformer weight vector. Simulation results are presented to show the effectiveness of the proposed algorithm for array configurability in the case of both

single and general rank signal correlation matrices. Performance comparisons between the proposed sparse array and uniform arrays as well as arrays without full augmentability constraint are provided.

1.2 Optimum Sparse Subarray Design for Multitask Receivers

The problem of optimum sparse array configuration to maximize the beamformer output signal-to-interference plus noise ratio (MaxSINR) in the presence of multiple sources of interest (SOI) has been recently addressed in the literature. In this report, we consider a shared aperture system where optimum sparse subarrays are allocated to individual SOIs and collectively span the entire full array receiver aperture. Each subarray may have its own antenna type and can comprise a different number of antennas. The optimum joint sparse subarray design for shared aperture based on maximizing the sum of the subarray beamformer SINRs is considered with and without SINR threshold constraints. We utilize Taylor series approximation and sequential convex programming (SCP) techniques to render the initial non-convex optimization a convex problem. The simulation results validate the shared aperture design solutions for MaxSINR for both cases where the number of sparse subarray antennas is predefined or left to comstitute an optimization variable.

2. List of Publications

Journals

[1] A. Hamza and **M. G. Amin**, "Hybrid sparse array beamforming design for general rank signal models," submitted to the IEEE Transactions on Signal Processing, June 2018.

[2] A. Deligiannis, **M. G. Amin**, S. Lambotharan, and G. Fabrizio, "Optimum sparse subarray design for multitask receivers," Under Review by IEEE Transactions on Aerospace and Electronic Systems.

Conferences

[3] A. Deligiannis, **M. G. Amin**, G. Fabrizio, and S. Lambotharan, "Optimum configurations of sparse subarray beamformers," Proceedings of the IEEE International Conference on Acoustics, Speech, and Signal Processing, Calgary, Alberta, Canada, April 2018.

[4] S. A. Hamza, **M. G. Amin** and G. Fabrizio, " Optimum sparse array design for maximizing signal-to-noise ratio in presence of local scatterings," Proceedings of the IEEE International Conference on Acoustics, Speech, and Signal Processing, Calgary, Alberta, Canada, April 2018.

[5] A. Deligiannis, **M. G. Amin**, G. Fabrizio, S. Lambotharan, "Sparse subarray design for multitask receivers," Proceedings of the IEEE Radar Conference, Oklahoma City, OK, April 2018.

[6] S. A. Hamza, **M. G. Amin** and G. Fabrizio," Optimum sparse array beamforming for general rank signal models,'' Proceedings of the IEEE Radar Conference, Oklahoma City, OK, April 2018.

3. Technical Description

3.1. Hybrid Sparse Array Beamforming Design for General Rank Signal Models

1. Introduction

Sparse array design through sensor selection reduces system overhead by lowering the hardware costs and processing complexity. It finds applications in sensor signal processing for communications, radar, sonar, satellite navigation, radio telescopes, speech enhancement and ultrasonic imaging [3, 9, 12, 14, 16, 17, 25]. One primary goal in these applications is to determine sensor locations to achieve optimality for some pre-determined performance criteria. The latter include minimizing the mean radius of the confidence ellipsoid associated with the estimation error covariance matrix [14] and Cramer Rao bound (CRB) to enhance the estimation accuracy for nonlinear measurement models that occur frequently in target parameter estimation, detection and tracking [6]. The performance of the design criteria depends largely on the operating environment, which may change according to the time-varying channel model assumed. This is in contrast to sparse arrays whose configurations follow certain formulas and seek to attain high extended aperture co-arrays. The driving objective, in this case, is to enable direction of arrival (DOA) estimation of more sources than physical sensors. Common examples are structured arrays such as nested and coprime arrays [18, 20, 22].

Sparse array design involves the selection of a subset of uniform grid points for sensor placements. For a given number of sensors, it is often assumed that the number of grid points, spaced by half wavelength, is unlimited. However in many applications, there is a constraint on the spatial extent of the system aperture. In this case, and depending on the number of sensors employed, a structured array may find itself placing the given sensors outside the available physical aperture. The problem then becomes of dual constraints, one relates to the number of sensors, and the other to the number of grid-points. With limited aperture constraint invoked, few sensors can be sufficient to produce a desirable filled structured co-array. Any additional sensors, in essence, constitute a surplus which can be utilized to meet an environment-dependent performance criterion, such as maximum signal-to-interference and noise ratio (SINR). In so doing, one can reap the benefits of structured and non-structured arrays. This paradigm calls for a

new aperture design approach which strives to provide filled co-arrays and at the same time be environment-sensitive. This hybrid design approach is the core contribution of this report.

Signal power estimation and enhancement in an interference active environment is an important and ubiquitous task in array signal processing. This problem has a direct bearing on improving target detection and localization for radar signal processing, increasing throughput or channel capacity for MIMO wireless communication systems, and enhancing resolution capability in medical imaging [10, 15, 30]. With sparse array, capon beamforming must not only find the optimum weights but also the optimum array configuration. This is an entwined optimization problem, and requires finding maximum SINR over all possible sparse array configurations. Maximum signal to noise ratio (MaxSNR) and MaxSINR have been shown to yield significantly efficient beamforming with its performance depending mainly on the positions of the sensors as well as the locations of sources in the field of view (FOV) [26, 28, 31].

In this report, we consider a bi-objective optimization problem, namely achieving the filled co-array and maximizing the SINR. The proposed technique enjoys three key advantages as compared to state-of-the-art sparse aperture design, namely, (a) It does not require any a priori knowledge of the correlated noisy environment i.e. jammers directions of arrival and their respective power which is implicitly assumed in the previous contributions [32, 33]; (b) It works directly on the received data correlation matrix and does not require the interference plus noise correlation matrix, which is not possible to estimate in many applications of sensor array processing [15, 27]; (c) It extends to spatial spread sources in a straightforward way.

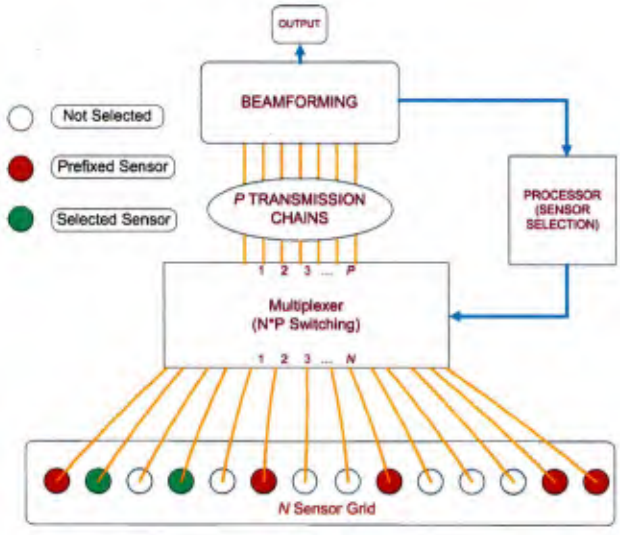

Figure 1: Block diagram of adaptive switched sensor beamforming

The proposed hybrid approach first determines a prefixed sparse array that results in a filled co-array with minimum number of sensors. This prefixed configuration could be a minimum redundancy array (MRA) [18], nested or coprime array configuration that fills the aperture under consideration with minimal sensors leaving behind maximum degrees of freedom for SINR maximization. This prefixed sensors configuration can be achieved by an optimization problem involving the minimum number of sensors spanning a pre-determined aperture. However, for the scope of this report, the prefixed configuration is determined by MRA or structured array indicating the sensor positions corresponding to the desired aperture. The remaining sensors after forming the prefixed array are then utilized to maximize the SINR. The cascade nature of the proposed hybrid approach is in lieu of the optimum design approach, which requires joint optimization of selecting the optimum filled sparse array that maximizes SINR. Environment dependent array design lowers the hardware complexity by reducing the expensive transmission chains through sensor switching as shown in the block diagram of the switched sensor beamforming in Fig. 1. The proposed hybrid approach, however, has an advantage of offering a simplified sensor switching in time-varying environment. This is attributed to the fact that there is a large number of fixed location sensors which would remain non-switched, irrespective of the sources and interferences in the FOV.

The proposed approach is also not particularly restrictive. To further clarify, it is noted that sparse arrays having N available sensors can typically span a filled array aperture of the order of $\mathcal{O}(N(N-1)/2)$; conversely, given an aperture spanning N possible sensor locations, only $\mathcal{O}(N^{1/2})$ sensors are sufficient to synthesize a fully augmentable array design. This emphasizes the fact that as the possible aperture size increases, then relatively few sensors are required to meet the full augmentability condition, possibly leaving many degrees of freedom to optimize for SINR enhancement. It should be noted that fully augmentable arrays not only provide the benefits of high resolution and improved identifiability of large number of sources, but also they ensure the availability of full array data covariance matrix essential to carry optimized SINR configuration [2], [1]. Moreover, the proposed approach lends itself to more desirable beampattern characteristics by maintaining minimum spacing between sensor elements.

We consider the problem of MaxSINR sparse arrays with limited aperture for both single and higher rank signal correlation matrices. The case of single rank correlation matrix arises when there is one desired source signal in the FOV, whereas the case of higher rank signal model occurs

for multiple point sources. We show the importance of sparse array configurability in both of the above cases by comparing the hybrid designed sparse array with the optimum sparse array configuration without the augmentability constraint and the commonly used compact ULA and rectangular arrays.

The problem is posed as optimally selecting P sensors out of N possible equally spaced grid points. Maximizing SINR amounts to maximizing the principal eigenvalue of the product of the inverse of data correlation matrix and the desired source correlation matrix [27]. Since it is an NP hard optimization problem, we pose this problem as QCQP with weighted l_1-norm squared to promote sparsity. The re-weighted l_1-norm convex relaxation has been exploited before for sensor selection problem for beampattern synthesis [7, 8], whereas, it is shown that the re-weighted l_1-norm squared relaxation is effective for reducing the required sensors and minimizing the transmit power for multicast beamforming [17]. We adopt a modified weighting matrix based iterative approach to control the sparsity of the optimum weight vector so that P sensor fully augmentable hybrid array is finally selected. This modified regularization weighting matrix based approach incorporates the prefixed structured array assumption in our design and works by minimizing the objective function around the presumed prefixed array.

The rest of the report is organized as follows: In the next section, we state the problem formulation for maximizing the output SINR under general rank signal correlation matrix. Section 3 deals with the optimum sparse array design by semidefinite relaxation and proposed modified re-weighting based iterative algorithm of finding P sensor fully augmentable hybrid sparse array design. In section 4, with the aid of number of design examples, we demonstrate the usefulness of fully augmentable arrays achieving MaxSINR and highlight the effectiveness of the proposed methodology for sparse array design. Concluding remarks follow at the end.

2. Problem Formulation

Consider K desired sources and L independent interfering source signals impinging on a linear array with N uniformly placed sensors. The baseband signal received at the array at time instant t is then given by;

$$\mathbf{x}(t) = \sum_{k=1}^{K} (\alpha_k(t))\mathbf{s}(\theta_k) + \sum_{l=1}^{L} (\beta_l(t))\mathbf{v}(\theta_l) + \mathbf{n}(t), \quad (1)$$

where, $\mathbf{s}(\theta_k)$ and $\mathbf{v}(\theta_l) \in \mathbb{C}^N$ are the corresponding steering vectors respective to directions of arrival, θ_k or θ_l, and are defined as follows;

$$\mathbf{s}(\theta_k) = [1 \quad e^{j(2\pi/\lambda)dcos(\theta_k)} \dots e^{j(2\pi/\lambda)d(N-1)cos(\theta_k)}]^T. \tag{2}$$

The inter-element spacing is denoted by d, $(\alpha_k(t),\ \beta_l(t)) \in \mathbb{C}$ denote the complex amplitudes of the incoming baseband signals [29]. The additive Gaussian noise $\mathbf{n}(t) \in \mathbb{C}^N$ has a variance of σ_n^2 at the receiver output. The received signal vector $\mathbf{x}(t)$ is combined linearly by the N-sensor beamformer that strives to maximize the output SINR. The output signal $y(t)$ of the optimum beamformer for maximum SINR is given by [27],

$$y(t) = \mathbf{w_0}^H \mathbf{x}(t), \tag{3}$$

where $\mathbf{w_0}$ is the solution of the optimization problem given below;

$$\begin{aligned} \underset{\mathbf{w}}{\text{minimize}} \quad & \mathbf{w}^H \mathbf{R}_{s'} \mathbf{w}, \\ \text{s.t.} \quad & \mathbf{w}^H \mathbf{R}_s \mathbf{w} = 1. \end{aligned} \tag{4}$$

For statistically independent signals, the desired source correlation matrix is given by, $\mathbf{R_s} = \sum_{k=1}^{K} \sigma_k^2 \mathbf{s}(\theta_k)\mathbf{s}^H(\theta_k)$, where, $\sigma_k^2 = E\{\alpha_k(t)\alpha_k^H(t)\}$. Likewise, we have the interference and noise correlation matrix $\mathbf{R_{s'}} = \sum_{l=1}^{L} (\sigma_l^2 \mathbf{v}(\theta_l)\mathbf{v}^H(\theta_l)) + \sigma_n^2 \mathbf{I}_{N*N}$, with $\sigma_l^2 = E\{\beta_l(t)\beta_l^H(t)\}$ being the power of the lth interfering source. The problem in (4) can be written equivalently by replacing $\mathbf{R_{s'}}$ with the received data covariance matrix, $\mathbf{R_{xx}} = \mathbf{R_s} + \mathbf{R_{s'}}$ as follows [27],

$$\begin{aligned} \underset{\mathbf{w}}{\text{minimize}} \quad & \mathbf{w}^H \mathbf{R}_{xx} \mathbf{w}, \\ \text{s.t.} \quad & \mathbf{w}^H \mathbf{R}_s \mathbf{w} = 1. \end{aligned} \tag{5}$$

There exists a closed form solution of the above optimization problem and is given by $\mathbf{w_0} = \mathcal{P}\{\mathbf{R_{s'}}^{-1}\mathbf{R_s}\} = \mathcal{P}\{\mathbf{R_{xx}}^{-1}\mathbf{R_s}\}$. The operator $\mathcal{P}\{.\}$ computes the principal eigenvector of the input matrix. Substituting $\mathbf{w_0}$ into (3) yields the corresponding optimum output SINR;

$$\text{SINR}_o = \frac{\mathbf{w_0^H R_s w_0}}{\mathbf{w_0^H R_{s'} w_0}} = \Lambda_{max}\{\mathbf{R_{s'}^{-1}R_s}\}. \tag{6}$$

Eq. (6) shows that the optimum output SINR (SINR_o) is given by the maximum eigenvalue

(Λ_{max}) associated with the product of the inverse of interference plus noise correlation matrix and the desired source correlation matrix. Therefore, the performance of the optimum beamformer for maximizing the output SINR is directly related to the desired and interference plus noise correlation matrix. It is to be noted that the rank of the desired source signal correlation matrix equals K, i.e. the cardinality of the desired sources.

3. Optimum sparse array design

The problem of locating the maximum principal eigenvalue among all the correlation matrices associated with P sensor selection is a combinatorial optimization problem. The constraint optimization (5) can be re-formulated for optimum sparse array design by incorporating an additional constraint on the cardinality of the weight vector;

$$\begin{aligned} \underset{\mathbf{w}\in\mathbb{C}^N}{\text{minimize}} \quad & \mathbf{w}^H\mathbf{R}_{xx}\mathbf{w}, \\ \text{s.t.} \quad & \mathbf{w}^H\mathbf{R}_s\mathbf{w} = 1, \\ & ||\mathbf{w}||_0 = P. \end{aligned} \tag{7}$$

Here, $||.||_0$ determines the cardinality of the weight vector $\mathbf{w}$. We assume that we have an estimate of all the filled co-array correlation lags corresponding to the correlation matrix of the full aperture array. The problem expressed in Eq. (7) can be relaxed to induce the sparsity in the beamforming weight vector $\mathbf{w}$ without placing a hard constraint on the specific cardinality of $\mathbf{w}$, as follows;

$$\begin{aligned} \underset{\mathbf{w}\in\mathbb{C}^N}{\text{minimize}} \quad & \mathbf{w}^H\mathbf{R}_{xx}\mathbf{w} + \mu(||\mathbf{w}||_1), \\ \text{s.t.} \quad & \mathbf{w}^H\mathbf{R}_s\mathbf{w} = 1. \end{aligned} \tag{8}$$

Here, $||.||_1$ is the sparsity inducing l_1-norm and μ is a parameter to control the desired sparsity in the solution. Even though the relaxed problem expressed in Eq. (8) is not exactly similar to that of Eq. (7), yet it is well known that l_1-norm regularization has been an effective tool for recovering sparse solutions in many diverse formulations. The problem in (8) can be penalized instead by the weighted l_1-norm function which is a well known sparsity promoting formulation [5],

$$\begin{aligned} \underset{\mathbf{w}\in\mathbb{C}^N}{\text{minimize}} \quad & \mathbf{w}^H\mathbf{R}_{xx}\mathbf{w} + \mu(||(\mathbf{b}^i \circ |\mathbf{w}|)||_1), \\ \text{s.t.} \quad & \mathbf{w}^H\mathbf{R}_s\mathbf{w} = 1. \end{aligned} \tag{9}$$

where, $'\circ'$ denotes the element wise product, $|.|$ is the modulus operator and $\mathbf{b}^i \in \mathbb{R}^N$ is the regularization weighting vector at the ith iteration. The weighted l_1-norm function in (9) is replaced by the l_1-norm squared function which does not alter the regularization property of the weighted l_1-norm function [17],

$$\begin{aligned} \underset{\mathbf{w}\in\mathbb{C}^N}{\text{minimize}} \quad & \mathbf{w}^H\mathbf{R}_{xx}\mathbf{w} + \mu(||(\mathbf{b}^i \circ |\mathbf{w}|)||_1^2), \\ \text{s.t.} \quad & \mathbf{w}^H\mathbf{R}_s\mathbf{w} = 1. \end{aligned} \tag{10}$$

The semidefinite formulation (SDP) of the above problem can then be realized by re-expressing the quadratic form, $\mathbf{w}^H\mathbf{R}_{xx}\mathbf{w} = \text{Tr}(\mathbf{w}^H\mathbf{R}_{xx}\mathbf{w}) = \text{Tr}(\mathbf{R}_{xx}\mathbf{w}\mathbf{w}^H) = \text{Tr}(\mathbf{R}_{xx}\mathbf{W})$, where Tr(.) is the trace of the matrix. Similarly, the regularization term $||(\mathbf{b}^i \circ |\mathbf{w}|)||_1^2 = (|\mathbf{w}|^T\mathbf{b}^i)((\mathbf{b}^i)^T|\mathbf{w}|) = |\mathbf{w}|^T\mathbf{B}^i|\mathbf{w}| = \text{Tr}(\mathbf{B}^i|\mathbf{W}|)$. Here, $\mathbf{W} = \mathbf{w}\mathbf{w}^\mathbf{H}$ and $\mathbf{B}^i = \mathbf{b}^i(\mathbf{b}^i)^T$ is the regularization weighting matrix at the ith iteration. Utilizing these quadratic expressions in (10) yields the following problem [4, 11, 17],

$$\begin{aligned} \underset{\mathbf{W}\in\mathbb{C}^{N*N},\widetilde{\mathbf{W}}\in\mathbb{R}^{N*N}}{\text{minimize}} \quad & \text{Tr}(\mathbf{R}_{xx}\mathbf{W}) + \mu\text{Tr}(\mathbf{B}^i\widetilde{\mathbf{W}}), \\ \text{s.t.} \quad & \text{Tr}(\mathbf{R}_s\mathbf{W}) \geq 1, \\ & \widetilde{\mathbf{W}} \geq |\mathbf{W}|, \\ & \mathbf{W} \succcurlyeq 0, \text{Rank}(\mathbf{W}) = 1. \end{aligned} \tag{11}$$

Here, $\geq$ is the element wise comparison and $\succcurlyeq$ denotes the inequality in the matrix sense. The rank constraint in Eq. (11) is non convex and therefore need to be removed. The rank relaxed approximation works well for the underlying problem. In case, the solution matrix is not rank 1, we can resort to randomization to harness rank 1 approximate solutions [23]. Alternatively, one could minimize the nuclear norm of $\mathbf{W}$, as a surrogate for l_1-norm in the case of matrices, to induce sparsity in the eigenvalues of $\mathbf{W}$ and promote rank one solutions [19, 24]. The resulting rank relaxed semidefinite program (SDR) is given by;

$$\begin{aligned} \underset{\mathbf{W}\in\mathbb{C}^{N*N},\widetilde{\mathbf{W}}\in\mathbb{R}^{N*N}}{\text{minimize}} \quad & \text{Tr}(\mathbf{R}_{xx}\mathbf{W}) + \mu\text{Tr}(\mathbf{B}^i\widetilde{\mathbf{W}}), \\ \text{s.t.} \quad & \text{Tr}(\mathbf{R}_s\mathbf{W}) \geq 1, \\ & \widetilde{\mathbf{W}} \geq |\mathbf{W}|, \\ & \mathbf{W} \succcurlyeq 0. \end{aligned} \tag{12}$$

In general, QCQP is NP hard and cannot be solved in polynomial time. The semidefinite relaxation of Eq. (12) is convex as all the correlation matrices involved are guaranteed to be positive semidefinite.

3.1 Fair gain beamforming

The optimization in Eq. (12) strives to incorporate the signal from all the directions of interest while optimally removing the interfering signals. To achieve this objective the optimum sparse array may show leaning towards a certain source of interest, consequently, not offering fair gain towards all sources. In an effort to promote equal gain towards all sources, we put a separate constraint on the power towards all desired sources as follows;

$$\begin{aligned} \underset{\mathbf{W}\in\mathbb{C}^{N*N},\widetilde{\mathbf{W}}\in\mathbb{R}^{N*N}}{\text{minimize}} \quad & \mathrm{Tr}(\mathbf{R}_{xx}\mathbf{W}) + \mu \mathrm{Tr}(\mathbf{B}^{i}\widetilde{\mathbf{W}}), \\ \text{s.t.} \quad & \mathrm{Tr}(\mathbf{R}_{k}\mathbf{W}) \geq 1, \quad \forall k \in (1,2,3\ldots K) \\ & \widetilde{\mathbf{W}} \geq |\mathbf{W}|, \\ & \mathbf{W} \succcurlyeq 0. \end{aligned} \tag{13}$$

Here, $\mathbf{R}_k = \mathbf{s}(\theta_k)\mathbf{s}^H(\theta_k)$ is the rank 1 covariance matrix associated with the source at DOA (θ_k). The feasible region of the above mentioned formulation is outside of the intersection of K ellipsoids associated with the inequality power constraints. This makes the solution of the underlying non relaxed QCQP challenging. However, the above SDR can be solved to an arbitrary small accuracy ζ, by employing interior point methods involving the worst case complexity of $\mathcal{O}\{\max(K,N)^4 N^{(1/2)}\log(1/\zeta)\}$ [23].

ALGORITHM 1	Proposed algorithm to achieve desired cardinality of optimal weight vector $\mathbf{w_0}$.
INPUT	Data correlation matrix $\mathbf{R}_{xx}$, N, P, look direction DOA's θ_k, selection vector $\mathbf{z}$.
OUTPUT	P sensor beamforming weight vector $\mathbf{w_0}$,
Initialization: Calculate the regularization weighting matrix $\mathbf{B} = \mathbf{z}\mathbf{z}^T$. In case of optimum array design without the augmentability constraint, initialize the selection vector $\mathbf{z}$ to be all ones vector.	
Initialize μ, ε.	

While (Sparsity is not invoked in $|\widetilde{\mathbf{W}}|$)

{

Run the SDR of Eq. (12).

Update the regularization weighting matrix $\mathbf{B}$ according to Eq. (15).

Binary search for desired cardinality P

$l = \mu_{lower}$, $u = \mu_{upper}$ (Initializing lower and upper limits of sparsity parameter range)

While (Cardinality of $\mathbf{w_0} \neq P$)

$\mu = [(l + u)/2]$

Run the SDR of Eq. (12) with the last regularization weighting matrix B from the previous while loop.

IF (Cardinality of $\mathbf{w_0}$) $< P$

$u = \mu$

Else

$l = \mu$

After achieving the desired cardinality, run SDP for reduced size correlation matrix corresponding to nonzero values of $\widetilde{\mathbf{W}}$ and $\mu = 0$, yielding, $\mathbf{w_0} = \mathcal{P}\{\mathbf{W}\}$.

3.2 Modified re-weighting for fully augmentable hybrid array

For the case without the full augmentability constraint the regularization weighting matrix $\mathbf{B}$ is initialized unweighted i.e. by all ones matrix and the m,nth element of $\mathbf{B}$ is iteratively updated as follows,

$$\mathbf{B}_{m,n}^{i+1} = \frac{1}{|\mathbf{W}_{m,n}^{i}| + \varepsilon}. \tag{14}$$

The parameter ε avoids the unwanted case of division by zero, though its choice is fairly independent to the performance of the iterative algorithm but at times very small values of ε can result in the algorithm getting trapped in the local minima [5]. For the hybrid array design, we initialize the weighting matrix instead as an outer product of selection vector $\mathbf{z}$. The selection vector $\mathbf{z}$ is an N dimensional vector containing binary entries of zero and one, where, zeros correspond to the pre-selected sensors and ones correspond to the remaining sensors to be selected.

Hence, the cardinality of $\mathbf{z}$ is equal to the difference of the total number of available sensors and the number of pre-selected sensors. This modified re-weighting approach ensures that the sensors corresponding to the pre-selected configuration is not penalized as part of the regularization, hence, $\mathbf{B} = \mathbf{z}\mathbf{z}^T$, thrives solutions that incorporate the pre-selected array topology. The modified penalizing weight update for the hybrid array design can be expressed as;

$$\mathbf{B}^{i+1} = (\mathbf{z}\mathbf{z}^T)(|\mathbf{W}^i| + \varepsilon). \tag{15}$$

The symbol denotes element wise division. The pseudo-code for controlling the sparsity of the optimal weight vector $\mathbf{w_0}$ is summarized in the TABLE (Algorithm 3.1).

3.3 Symmetric arrays

The solution of the SDR formulation is penchant for symmetric arrays in the case of symmetric initialization vector $\mathbf{z}$. The plausible explanation is as follows. We first show that the beamforming weights which maximizes the output SINR for symmetric sparse array topologies are conjugate symmetric w.r.t. the array center.

Proposition 1 *The conjugate symmetry of the optimal weight vector holds for centro-symmetric sparse array configurations in case of the general rank desired source model.*
Proof. (Refer to the Appendix for the proof.)

We observe that the regularized cost function does not invoke sparsity until after the first few initial iterations. Consequently, the initial solutions of the semidefinite program has symmetric coefficients as the SDR seeks near optimal solutions which are analytically shown to be conjugate symmetric. Moreover, the iterative sparsity enhancing formulation introduces sparsity by penalizing the beamforming weight vector according to Eq. (15), where, it only accounts the magnitude of the beamforming weights. Therefore, at each iteration the regularization weighting matrix $\mathbf{B}$ happens to penalize the solution weight vector in a symmetric fashion around the array center. Thus, the iterative SDR sparse solution favors symmetric configurations by discarding corresponding symmetric sensors simultaneously. Though, the symmetric configuration can be desirable for certain applications and can have desirable performance, yet, it reduces the available degrees of freedom. Therefore, to circumvent this problem, we couple the modified re-weighting

approach with greedy sensor selection type methodology that works by discarding only one sensor at a time if more than one sensors are eliminated simultaneously by the algorithm. The sensor which has the inferior objective function performance is discouraged in the design by utilizing the methodology explained in 3.2 with a subtle modification. In the case of the hybrid array design, we prefixed sensors in our design a priori by setting regularization weights to be zero corresponding to the pre-selected sensors. In contrary over here, we set the corresponding regularization weight to be relatively high for the specific sensor that needs to be discouraged, thereby resolving issues arising from the symmetric regularization weighting matrix.

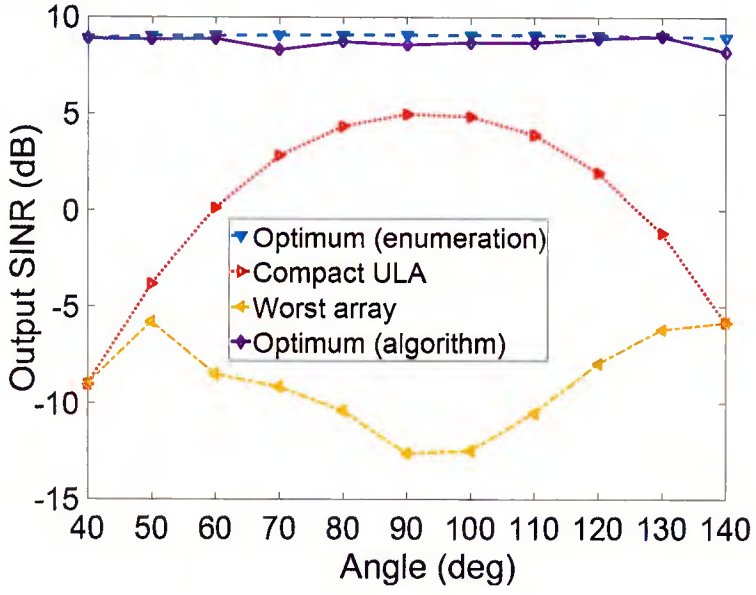

Figure 2: Output SINR for different array topologies

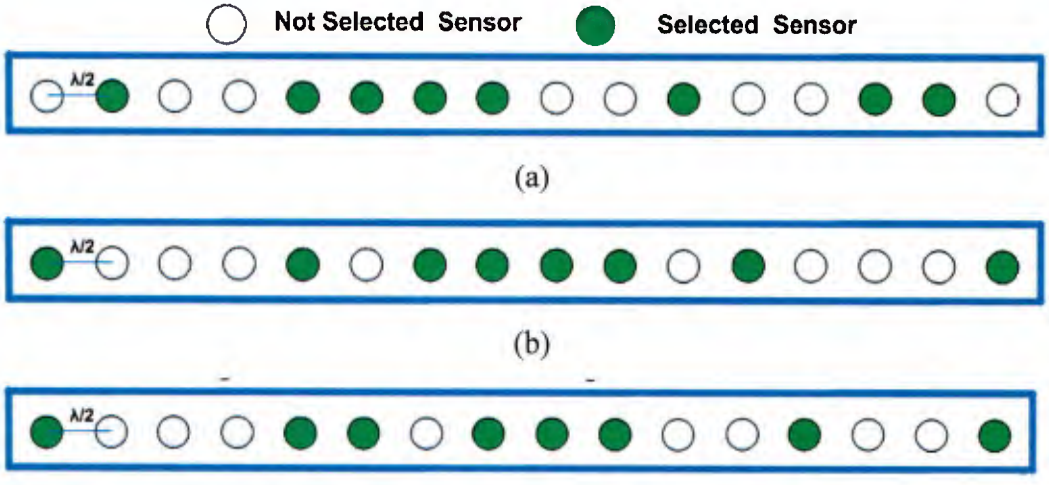

(c)

(d)

Figure 3: Array configurations obtained for the point source at the array broadside (a) Optimum (enumeration) (b) Optimum (algorithm) (c) Symmetric design consideration according to Section 3.3 (d) Worst performing array configuration

4 Simulations

In this section, we show the effectiveness of the proposed technique for the sparse array design for MaxSINR. We initially test this proposed approach for array configurability by considering arbitrary arrays without the augmentability constraint. In the later examples, we demonstrate the effectiveness of fully augmentable hybrid sparse array design through linear and 2D arrays. We focus on the EM modality, and as such we use antennas for sensors.

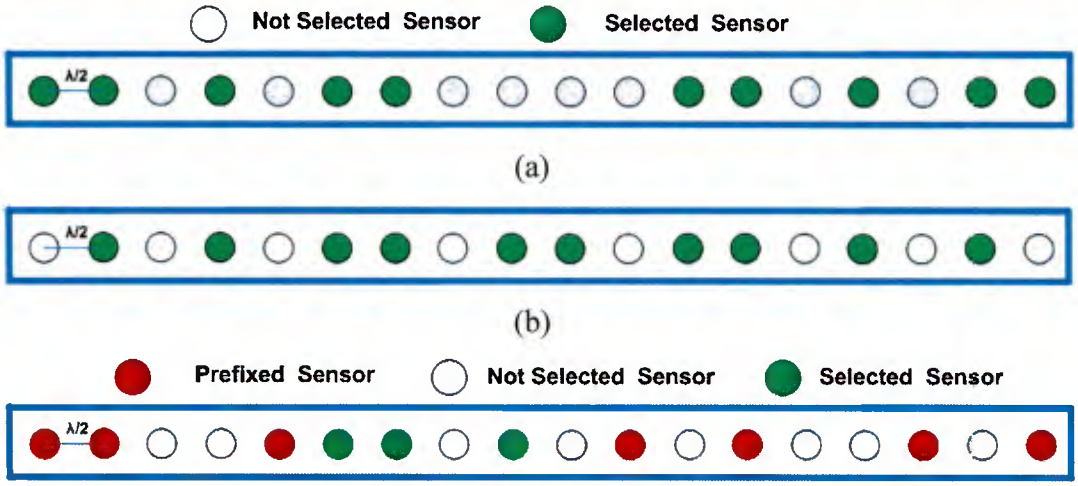

Figure 4: (a) Optimum 10 element antenna array multiple sources (algorithm) (b) Fair gain 10 antenna array (c) Hybrid design 10 antenna array for multiple desired sources

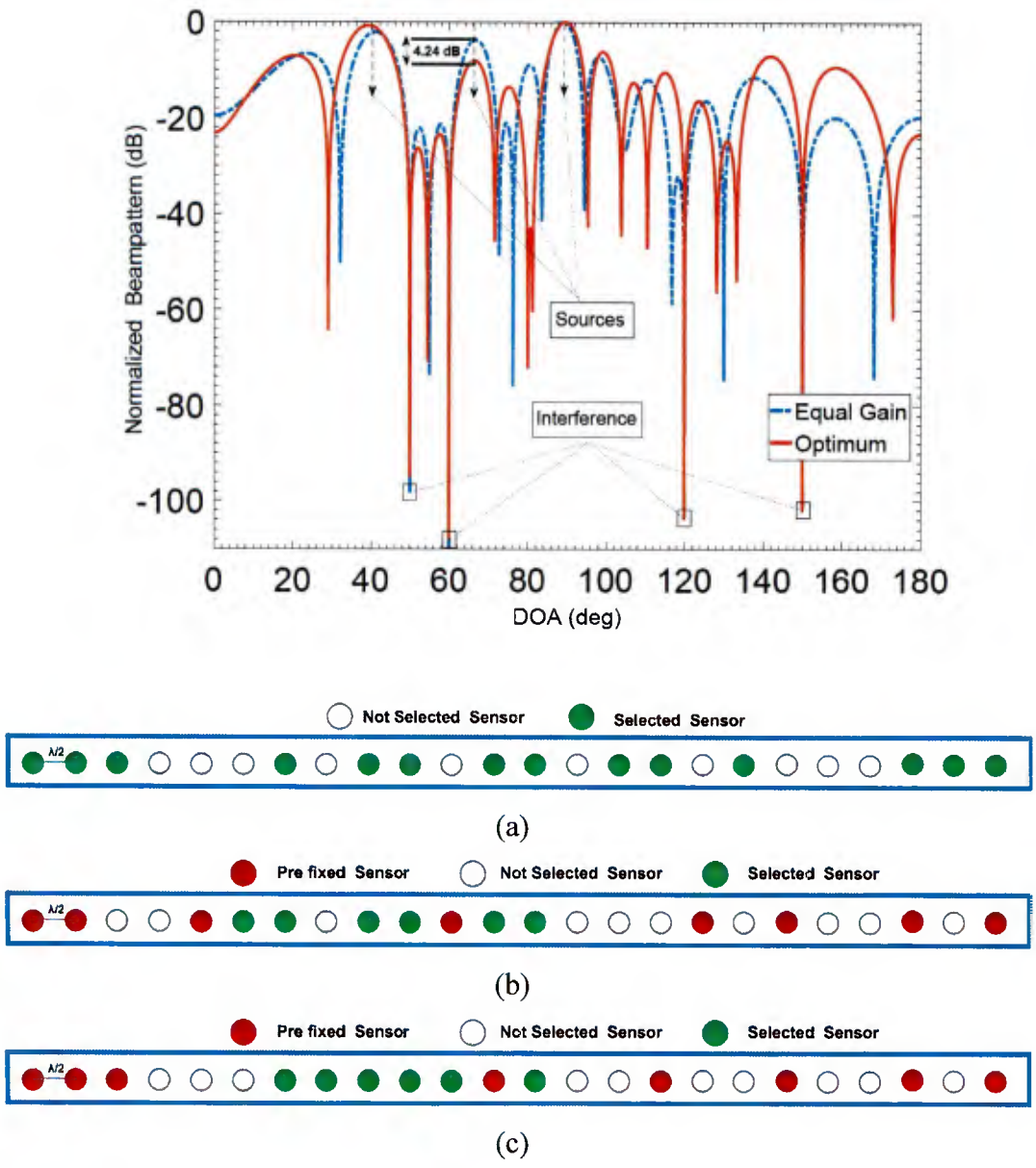

Figure 6: (a) Optimum 14 antenna sparse array (convex relaxation) (b) 14 antenna hybrid array (8 prefixed, 6 selected) (c) 14 antenna hybrid array (8 prefixed, 6 selected)

4.1 Single point source

We select $P = 8$ antennas from $N = 16$ possible equally spaced locations with inter-element spacing of $\lambda/2$. Figure 2 shows the output SINR for different array configurations for the case of single desired point source with its DOA varying from 40^0 to 140^0. The interfering

signals are located at 20^0 and $\pm 10^0$ degree apart from the desired source angle. To explain this scenario, suppose that the desired source is at 60^0, we consider the respective directions of arrival of the three interfering signals at 40^0, 50^0 and 70^0. The SNR of the desired signal is 0 dB, and the interference to noise ratio (INR) of interfering signals is set to 20 dB each. From the Fig. 2, it is evident that the proposed algorithm performs close to the performance of the optimum array found by exhaustive search (12870 possible configurations), which has very high computational cost attributed to expensive singular value decomposition (SVD) for each enumeration. On average, the proposed algorithm takes six to seven iterations to converge to the optimum antenna locations; hence, offering considerable savings in the computational cost. It is of interest to compare the optimum sparse array performance with that of compact ULA. It can be seen from Fig. 2, that the optimum sparse array offers considerable SINR advantage over the compact ULA for all source angles of arrival. The ULA performance degrades severely when the source of interest is more towards the array end-fire location. In this case, the ULA fails to resolve and cancel the strong interferers, while maintaining unit gain towards the source of interest. For the case of the desired source at the array broadside, the maximum output SINR of the optimum array found through enumeration is 9.03 dB. The optimum array design obtained through the proposed algorithm yields an output SINR of 8.6 dB, which is 0.4 dB less than the corresponding SINR of the optimum array found through exhaustive search. The broadside source arrays are shown in the Fig. 7 (where green-filled circle indicates antenna present whereas gray-filled circle indicates antenna absent). The sparse array recovered through proposed algorithm is clearly a symmetric configuration (Fig. 4). Figure 5 shows the sparse array found after addressing the symmetry bias by the approach explained in Section 3.3. The SINR for this non-symmetric configuration is 8.93 dB and is suboptimal merely by 0.1 dB. It is worth noticing that the worst performing sparse array configuration utilizes maximum array aperture (Fig. 6), yet it has an output SINR as low as -13 dB. This emphasizes the fact that if an arbitrary sparse array structure is employed, it could degrade the performance catastrophically irrespective of the occupied aperture and could perform far worst than the compact ULA, which offers modest output SINR of 5 dB for the scenario under consideration.

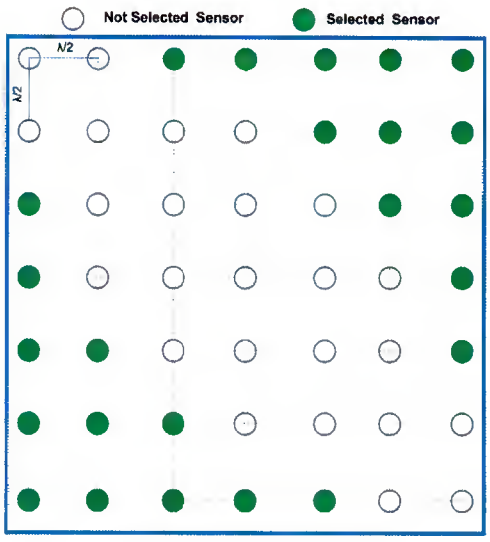

Figure 7: Optimum 24 element antenna sparse array (convex relaxation)

4.2 Multiple point sources

For the multiple point sources scenario, consider three desired signals impinging from DOAs 40^0, 65^0 and 90^0 with SNR of 0 dB each. Four strong interferers with INR of 30 dB each, are operational at DOAs 50^0, 60^0, 120^0 and 150^0. We select 10 antennas out of 18 available slots. The optimum array recovered through convex relaxation is shown in Fig. 8. This configuration results with an output SINR of 11.85 dB against SINR of 12.1 dB for the optimum configuration found through enumeration. For the fair gain beamforming, we apply the optimization of Eq. (13) and the array configuration for MaxSINR for the fair gain beamforming is shown in Fig 9. The output SINR for the fair beamforming case is 11.6 dB which is slightly less than the optimum array without the fair gain consideration (11.85 dB). However, the advantage of fair beamforming is well apparent from the beampatterns in both cases as shown in Fig (12), where the gain towards the source at 65^0 is around 4.24 dB higher than the case of optimum array without the fair gain consideration. The maximum gain deviation for the fair gain case is 3.5 dB vs. 8 dB variation without the fair gain consideration. The SINR of compact ULA is compromised more than 3 dB as compared to the optimum sparse array (Fig. 8) obtained through the proposed methodology. This improved performance is due to the optimum sparse array smartly engaging its degrees of freedom to eradicate the interfering signals while maintaining maximum gain towards all sources of interest.

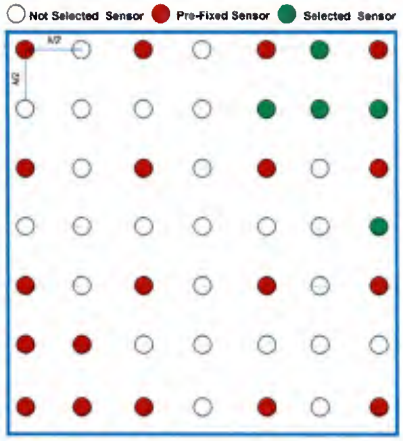

Figure 8: 24 element hybrid antenna array via convex relaxation (19 prefixed, 5 selected)

4.3 Fully augmentable linear arrays

Consider selecting 14 antennas out of 24 possible available locations with antenna spacing of $\lambda/2$. A desired source is impinging from DOA of 30^0 and SNR of 0 dB, whereas strong narrowband jammers are operating at 20^0, 40^0 and 120^0 with INR of 20 dB each. Optimum array configuration (Fig. 13) achieved through convex relaxation has an output SINR of 11.04 dB as compared to SINR of 11.32 dB of an optimum array recovered through enumeration ($1.96 * 10^6$ possible configurations). It should be noted that the array recovered without filled co-array constraint is not essentially fully augmentable as is the case in the optimum array (Fig. 13) which clearly has missing co-array lags.

In quest of fully augmentable array design we prefix 8 antennas (red elements in Fig. 14) in a minimum redundancy array (MRA) configuration over 24 uniform grid points. This provides 24 consecutive autocorrelation lags. We are, therefore, left with six antennas to be placed in the remaining 16 possible locations (8008 possible configurations). We enumerated the performance of all possible hybrid arrays associated with underlying MRA configuration and found the output SINR ranges from 8.06 dB to 11.3 dB. Figure 14 shows the configuration recovered through the proposed approach which has an output SINR of 10.96 dB. The proposed approach thus recovers the hybrid sparse array with performance close to the best possible, moreover it approximately yields 3 dB advantage over worst fully augmentable hybrid array. As MRAs are not unique we started with a different 8 element MRA structured array (red elements in Fig. 15), to further reinforce the effectiveness of fully augmentable sparse arrays. The dynamic performance range associated with MRA of Fig. 15, is from 7.54 dB to 11.3 dB. The performance in this case is very similar to the aforementioned MRA configuration with the output SINR of 10.7 dB

for the hybrid array recovered through proposed methodology (Fig. 15). The maximum possible SINR offered by both hybrid arrays is 11.3 dB which is extremely close to SINR performance of 11.32 dB offered by the optimum array without augmentability constraint. Furthermore, the compact ULA has an output SINR of 7.54 dB which is again considerably less than the hybrid sparse arrays. We also test the fully augmentable array design for the case of multiple point source scenario described previously (Section 4.2). The hybrid array recovered through proposed methodology is shown in the Fig. 10 (red elements showing the 7 element MRA). The output SINR is 11.566 dB and is sufficiently close to the performance achieved through enumeration.

4.4 Fully augmentable 2 D arrays

Consider a $7 * 7$ planar array with grid pacing of $\lambda/2$ where we place 24 antennas at 49 possible positions. A desired source is impinging from elevation angle $\theta = 50^0$ and azimuth angle of $\phi = 90^0$. Here, elevation angle is with respect to the plane carrying the array rather than reference from the zenith. Four strong interferes are impinging from $(\theta = 20^0, \phi = 30^0)$, $(\theta = 40^0, \phi = 80^0)$, $(\theta = 40^0, \phi = 105^0)$ and $(\theta = 35^0, \phi = 20^0)$. The INR corresponding to each interference is 20 dB and SNR is set to 0 dB. There are of the order of 10^{14} possible 24 antenna configurations, hence the problem is prohibitive even by exhaustive search. Therefore, we resort to the upper bound of performance limits to compare our results. Here, we utilize the fact that the best possible performance occurs when the interferes are completely canceled in the array output and the output SINR in that case would equal the array gain offered by the 24 element array

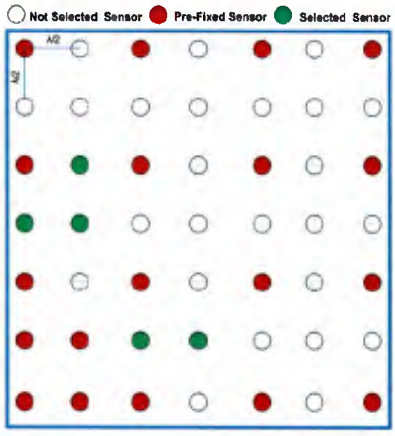

Figure 9: 24 element worst performing hybrid antenna array (19 prefixed, 5 selected)

which amounts to 13.8 dB. Figure 7 shows the optimum antenna locations recovered by our

algorithm. The output SINR for this configuration is 13.68 dB which is sufficiently close to the ideal performance. It should be noted that again the array recovered in the Fig. 7 is not fully augmentable as it is missing quiet a few correlation lags.

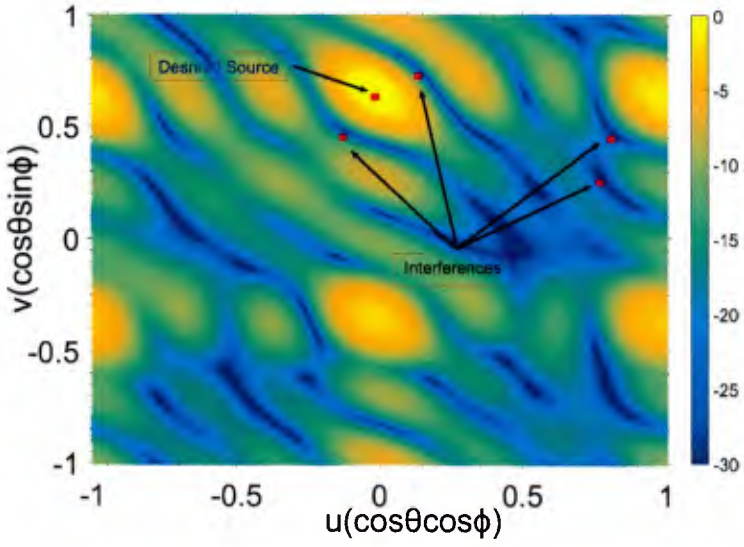

Figure 10: Beampattern for the antenna array in Fig. 8

We now introduce the condition of full augmentability by placing 19 antennas in nested lattice configuration [21] to form a filled co-array (red elements in Fig. 18). The rest of five available antennas can be placed in the remaining 30 possible locations hence resulting in approximately $1.5 * 10^5$ possibilities. Figure 18 shows the hybrid sparse geometry recovered by convex relaxation and offers SINR of 13.25 dB which is around 0.4 dB less than the optimum array. The performance range of the hybrid arrays associated with the structured nested lattice array ranges from 11.4 dB to 13.38 dB (found through exhaustive search). In this regard our proposed algorithm finds the hybrid sparse array with the performance degradation of little more than 0.1 dB. The worst performing hybrid array (Fig. 19) has an output SINR of 11.4 dB and is around 2 dB lower than the best performing hybrid sparse array.

It is of interest to compare the performance of aforementioned sparse arrays with a compact 2D array. For this purpose, we chose a $6 * 4$ rectangular array. The compact rectangular array performs very poorly in the underlying scenario and has an output SINR of 7.8 dB which is more than 5 dB down from the hybrid sparse array recovered through the semidefinite relaxation. This performance degradation is very clear from the beampattern of both arrays shown in Fig. 20 and 21 (normalized beampattern in dB). In the case of the hybrid sparse array recovered through SDR

(Fig. 18), the target has the maximum gain towards the direction of interest and it maintains minimum gain simultaneously towards all unwanted DOAs (Fig. 20). In contrast, it is clear from Fig. 21 that the beampattern of compact rectangular array could not manage maximum gain towards the direction of interest while effectively rejecting the interfering signals. The hybrid array also appears to be more robust as it has higher dynamic performance range threshold (11.4 dB), as it has been shown in previous examples that the performance of arbitrary arrays is more susceptible to deteriorate catastrophically even far worst than that of the compact uniform or rectangular arrays.

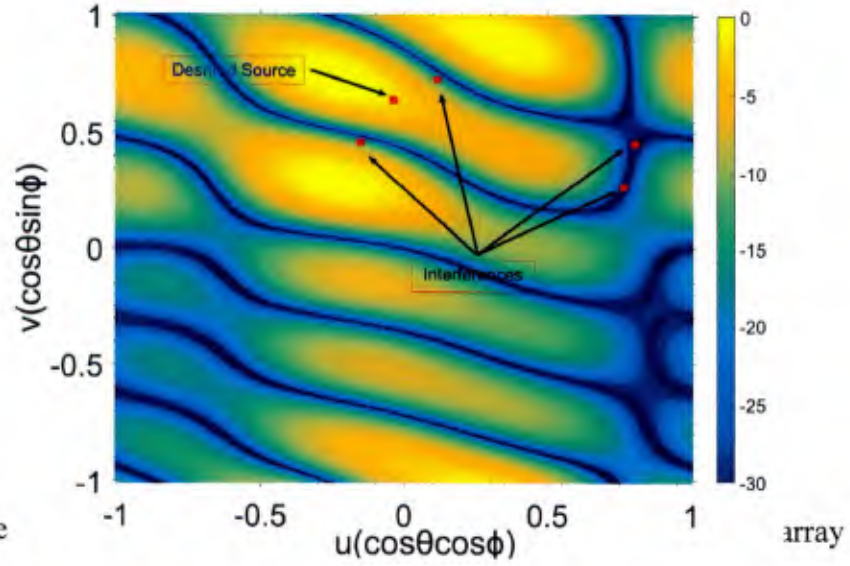

Figure array

5 Conclusion

This report considered fully augmentable sparse array configurations for maximizing the beamformer output SINR for general rank desired signal correlation matrices. It proposed a hybrid sparse array design that simultaneously considers co-array and environment-dependent objectives. This design potentially offers comparable SINR performances as compared to sparse arrays that are freely designed without the augmentability constraint. The proposed array design approach uses a subset of the available sensors to obtain a fully augmentable array while employing the remaining sensors for achieving the highest SINR. We applied the modified re-weighting QCQP which proved effective in recovering superior SINR performance for hybrid sparse arrays in polynomial run times. The proposed approach was extended for fair gain beamforming towards multiple sources. We solved the optimization problem by both the proposed algorithm and enumeration and showed strong agreement between the two methods.

Appendix: [Proof of the Conjugate symmetric property of optimal weight vector]

Proof. The correlation matrix $\mathbf{R}$ for centro-symmetric arrays have a conjugate persymmetric structure such that [13]:

$$\mathbf{TR'T} = \mathbf{R} \tag{16}$$

Here $\{'\}$ is the conjugate operator and $\mathbf{T}$ is the transformation matrix which flips the entries of a vector upside down by left multiplication;

$$\mathbf{T} = \begin{bmatrix} 0 & \dots & 0 & 0 & 1 \\ 0 & \dots & 0 & 1 & 0 \\ \vdots & \dots & & \vdots & \\ 1 & \dots & 0 & & 0 \end{bmatrix}$$

The optimal weight vector which maximizes the SINR is given by;

$$\mathbf{w_0} = \mathcal{P}\{\mathbf{R_{s'}}^{-1}\mathbf{R_s}\} \tag{17}$$

where,

$$\{\mathbf{R_{s'}}^{-1}\mathbf{R_s}\}\mathbf{w_0} = \Lambda_{max}\mathbf{w_0} \tag{18}$$

Using the relation in (16), Eq. (18) can be re-expressed as follows,

$$\begin{aligned} \{(\mathbf{TR'_{s'}T})^{-1}(\mathbf{TR'_sT})\}\mathbf{w_0} &= \Lambda_{max}\mathbf{w_0} \\ \{\mathbf{T}^{-1}(\mathbf{R'_{s'}})^{-1}\mathbf{T}^{-1}(\mathbf{TR'_sT})\}\mathbf{w_0} &= \Lambda_{max}\mathbf{w_0} \end{aligned} \tag{19}$$

Multiplying both sides by $\mathbf{T}$ and applying the conjugate operator,

$$\{\mathbf{R_{s'}}^{-1}\mathbf{R_s}\}\mathbf{Tw'_0} = \Lambda_{max}\mathbf{Tw'_0} \tag{20}$$

Eq. (20) shows that $\mathbf{Tw'_0}$ is also the principal eigenvector associated with matrix $\mathbf{R_{s'}}^{-1}\mathbf{R_s}$. Since the principal eigenvector of the positive definite hermitian matrix is unique up to the scalar complex multiplier, this directly implies that;

$$\mathbf{w_0} = \mathbf{Tw'_0}$$

References

[1] Y.I. Abramovich, N.K. Spencer, and A.Y. Gorokhov, "Positive-definite Toeplitz completion in DOA

estimation for nonuniform linear antenna arrays. II. Partially augmentable arrays, "*Trans. Sig. Proc.*, 47(6):1502–1521, June 1999.

[2] Y. I. Abramovich, D. A. Gray, A. Y. Gorokhov, and N. K. Spencer, "Positive-definite Toeplitz completion in DOA estimation for nonuniform linear antenna arrays. I. Fully augmentable arrays," *IEEE Transactions on Signal Processing*, 46(9):2458–2471, Sep 1998.

[3] W. a. V. Cappellen, S. J. Wijnholds, and J. D. Bregman, "Sparse antenna array configurations in large aperture synthesis radio telescopes," In *2006 European Radar Conference*, pages 76–79, Sept 2006.

[4] M. Bengtsson and B. Ottersten, "Optimal downlink beamforming using semidefinite optimization, 1999.

[5] E. J. Candès, M. B. Wakin, and S. P. Boyd, "Enhancing sparsity by reweighted l_1 minimization," *Journal of Fourier Analysis and Applications*, 14(5):877–905, Dec. 2008.

[6] S. P. Chepuri and G. Leus, "Sparsity-promoting sensor selection for non-linear measurement models," *IEEE Transactions on Signal Processing*, 63(3):684–698, Feb 2015.

[7] S. Eng Nai, W. Ser, Z. Yu, and H. Chen, "Beampattern synthesis for linear and planar arrays with antenna selection by convex optimization," 58:3923 – 3930, 01 2011.

[8] B. Fuchs, "Application of convex relaxation to array synthesis problems," *IEEE Transactions on Antennas and Propagation*, 62(2):634–640, Feb. 2014.

[9] H. Godrich, A. P. Petropulu, and H. V. Poor, "Sensor selection in distributed multiple-radar architectures for localization: A knapsack problem formulation, " *IEEE Transactions on Signal Processing*, 60(1):247–260, Jan 2012.

[10] A. Goldsmith. *Wireless Communications*. Cambridge University Press, New York, NY, USA, 2005.

[11] S. A. Hamza, M. G. Amin, and G. Fabrizio, "Optimum sparse array beamforming for general rank signal models, " *IEEE Radar Conference (RadarConf18)*, pages 1343–1347, April 2018.

[12] M. B. Hawes and W. Liu, "Sparse array design for wideband beamforming with reduced complexity in tapped delay-lines, " *IEEE/ACM Transactions on Audio, Speech, and Language Processing*, 22(8):1236–1247, Aug 2014.

[13] K. Huarng and C. The, "Adaptive beamforming with conjugate symmetric weights," *IEEE Transactions on Antennas and Propagation*, 39(7):926–932, July 1991.

[14] S. Joshi and S. Boyd, "Sensor selection via convex optimization, "*IEEE Transactions on Signal Processing*, 57(2):451–462, Feb 2009.

[15] J. Li, P. Stoica, and Z. Wang, "On robust capon beamforming and diagonal loading," *IEEE Transactions on Signal Processing*, 51(7):1702–1715, July 2003.

[16] G. R. Lockwood, J. R. Talman, and S. S. Brunke, "Real-time 3-D ultrasound imaging using sparse synthetic aperture beamforming, "*IEEE Transactions on Ultrasonics, Ferroelectrics, and Frequency Control*, 45(4):980–988, July 1998.

[17] O. Mehanna, N.D. Sidiropoulos, and G.B. Giannakis, "Joint multicast beamforming and antenna selection," *IEEE Transactions on Signal Processing*, 61(10):2660–2674, May 2013.

[18] A. Moffet, "Minimum-redundancy linear arrays," *IEEE Transactions on Antennas and Propagation*, 16(2):172–175, March 1968.

[19] K. Mohan and M. Fazel, "Iterative reweighted algorithms for matrix rank minimization," *J. Mach. Learn. Res.*, 13(1):3441–3473, November 2012.

[20] P. Pal and P.P. Vaidyanathan, "Nested arrays: A novel approach to array processing with enhanced degrees of freedom," *IEEE Transactions on Signal Processing*, 58(8):4167–4181, Aug. 2010.

[21] P. Pal and P. P. Vaidyanathan, "Nested arrays in two dimensions, Part 1: Geometrical considerations," *IEEE Transactions on Signal Processing*, 60(9):4694–4705, Sept 2012

[22] S. Qin, Y.*D* Zhang, and M.G. Amin, "Generalized coprime array configurations for direction-of-arrival estimation," *IEEE Transactions on Signal Processing*, 63(6):1377–1390, March 2015.

[23] Z. q. Luo, W. k. Ma, A. M. c. So, Y. Ye, and S. Zhang, "Semidefinite relaxation of quadratic optimization problems, "*IEEE Signal Processing Magazine*, 27(3):20–34, May 2010.

[24] Benjamin Recht, Maryam Fazel, and Pablo A. Parrilo. Guaranteed minimum-rank solutions of linear matrix equations via nuclear norm minimization. *SIAM Rev.*, 52(3):471–501, August 2010.

[25] W. Roberts, L. Xu, J. Li, and P. Stoica, "Sparse antenna array design for MIMO active sensing applications," *IEEE Transactions on Antennas and Propagation*, 59(3):846–858, March 2011.

[26] V. Roy, S.P. Chepuri, and G. Leus, "Sparsity-enforcing sensor selection for DOA estimation," *IEEE International Workshop on Computational Advances in Multi-Sensor Adaptive Processing (CAMSAP)*, pages 340–343, Dec. 2013.

[27] S. Shahbazpanahi, A. B. Gershman, Zhi-Quan Luo, and Kon Max Wong, "Robust adaptive beamforming for general-rank signal models, " *IEEE Transactions on Signal Processing*, 51(9):2257–2269, Sept. 2003.

[28] N.D. Sidiropoulos, T.N. Davidson, and Zhi-Quan Luo, "Transmit beamforming for physical-layer multicasting, "*IEEE Transactions on Signal Processing*, 54(6):2239–2251, June 2006.

[29] Petre Stoica and Randolph L Moses. *Introduction to spectral analysis*. Upper Saddle River, N.J. : Prentice Hall, 1997.

[30] Harry L. Van Trees. *Detection, Estimation, and Modulation Theory: Radar-Sonar Signal Processing and Gaussian Signals in Noise*. Krieger Publishing Co., Inc., Melbourne, FL, USA, 1992.

[31] X. Wang, E. Aboutanios, M. Trinkle, and M. G. Amin, "Reconfigurable adaptive array beamforming by antenna selection," *IEEE Transactions on Signal Processing*, 62(9):2385–2396, May 2014.

[32] X. Wang, M. G. Amin, X. Wang, and X. Cao, "Sparse array quiescent beamformer design combining adaptive and deterministic constraints," *IEEE Transactions on Antennas and Propagation*, PP(99):1–1, 2017.

[33] X. Wang, M. Amin, and X. Cao, "Analysis and design of optimum sparse array configurations for adaptive beamforming," *IEEE Transactions on Signal Processing*, PP(99):1–1, 2017.

3.2. Optimum Sparse Subarray Design for Multitask Receivers

1 Introduction

Shared aperture antenna describes a system of two or more sparse subarrays, each performing a separate task, deployed on a common aperture [29]. The subarray tasks are dependent on the system operation which could jointly support several required services. A 3D shared aperture antenna that supports different operating frequencies was proposed in [29]. The compound system consists of two stacked arrays, transmitting through the same aperture, the upper level operating in the L-band and being electrically isolated from the lower one that operates in the X-band. The coexistence of radar, electronic warfare and communications functions on the same aperture was investigated in [32], where subarrays with different operating frequencies and polarization are utilized to perform separate tasks. The design of a shared dual-band transmitting/receiving platform, where separated sparse subarrays of S-band and X-band elements are designed for simultaneous transmitting and receiving operation was investigated in [20]. Three different radar applications of a shared aperture antenna using interleaved sparse subarrays on a common platform were considered in [21], namely, multi-frequency shared aperture antenna, shared aperture antenna implementing polarisation agility and interleaved transmiting/receiving shared aperture antenna. The synthesis of linear multi-beam arrays on a shared aperture through hierarchical almost difference set (ADS)-based interleaving was studied in [26].

In this report, each sparse subarray of the shared aperture performs separate beamforming and strives to maximize the signal-to-interference and noise ratio (SINR) for its designated source or for a specific direction. Maximizing SINR at the receiver increases the probability of target detection in radar and reduces bit error rates in communications. In this respect, the different tasks assigned to the shared aperture antenna could belong to the same functionality, i.e., either radar or communication or across different functions as part of platform coexistence, i.e. joint radar communication system [15]. In either case, the system may mandate unshared antennas among the subarrays to reduce signal processing complexity and limit radar cross-sections. Moreover, the different tasks may demand antennas with diverse properties, polarization or bandwidth [20]. The beamformer output is not only affected by the antenna output multiplicative coefficients but also by the antenna array configuration [2, 31, 35]. Hence, optimal beamforming should utilize both the beampattern array coefficients as well as the array configuration [22, 23].

Optimal beamforming techniques efficiently mitigate the interference and noise at the output of the system while enhancing the response towards the sources of interest (SOI) [3, 6, 9, 10, 39], casting it as a powerful tool for many active and passive sensing applications, such as radar, sonar, wireless communications, radio telescope, ultrasound and seismology [5, 8, 13, 18, 25]. Sparse transmit array design for radiating shaped beamformers was investigated in [24] exploiting compressive sensing. Adaptive interference nulling techniques based on the appropriate selection of the array elements were proposed in [16, 28], utilizing genetic algorithms and SINR maximization, respectively. As demonstrated in [12, 37], sparse array configuration has a substantial impact on both the beamformer output signal-to-noise ratio (SNR) and SINR. Optimum adaptive sparse arrays for maximizing SNR (MaxSNR) and SINR (MaxSINR) are superior to structured sparse arrays such as coprime, nested and uniform arrays [37]. This is attributed to the fact that adaptive beamforming and sparse array design take into consideration the operating environment, by incorporating the source, interference and noise spatial and temporal characteristics in the optimization [7]. Most of the existing work on maxSINR beamforming focuses on a single mission array where the entire array aperture, regardless of whether it is full or sparse, is tasked to deal with one or more sources in the field of view (FOV) [38]. In such case, the main objective is to maximize the SINR at the output of the receiver by optimally configuring the array and deciding on the beamformer coefficients. This technique, is deemed to result in unequal SINR or SNR for the sources considered and does not guarantee an acceptable minimum SNR or SINR performance for any of the sources. Using a separate beamformer, along with its antennas and coefficients, for each source is a generalization of the above technique.

In this report, we investigate scenarios that fall into the aforementioned framework of multi-mission or multitask sensing of a shared aperture with separate, but complementing, sparse subarrays. That is, the combined subarrays make up the system aperture. The multiple sources considered are in the far field and may represent targets reflecting a transmitted waveform or active emitters, thus covering many scenarios including radar, wireless communications, electronic warfare and radio telescope. We propose a method for optimum design of antenna aperture comprising multiple sparse subarrays, each processes the signal from one source. The goal is to select the antenna positions and coefficients to jointly maximize the SINR for all sources. The optimum subarrays are obtained by performing a joint SINR optimization for matched MVDR beamforming. We examine both cases in which specific cardinality of antennas per subarray is set

a priori and when the number of antennas in each subarray is left as an optimization variable. By considering the cardinality as an optimization variable, we provide more design flexibility and additional degrees of freedom to the system, resulting in higher SINR performance, especially when dealing with high spatially correlated sources. The choice of SINR as a performance metric is motivated by the fact higher SINR enhances target detection in radar, and minimizes bit error rates in communications, leading to a better quality of service [11, 19, 30, 34]. We also propose a joint optimum sparse subarray design technique with the objective of maximizing the SINR of some sources, while attaining a predefined SINR threshold for the remaining sources. We utilize Taylor series approximation and sequential convex programming techniques to render the initially non-convex SINR optimization problems as convex. The rest of the report is organized as follows: The mathematical model of the system is formulated in section II. The sparse subarray design for both cases of given number of antennas per subarray and when the cardinality of antennas is a design variable is examined in section III. The SINR constrained optimum sparse subarray design is presented in section IV. Simulation results and remarks on the results are given in section V, and the final conclusions are drawn in section VI.

2 System Model

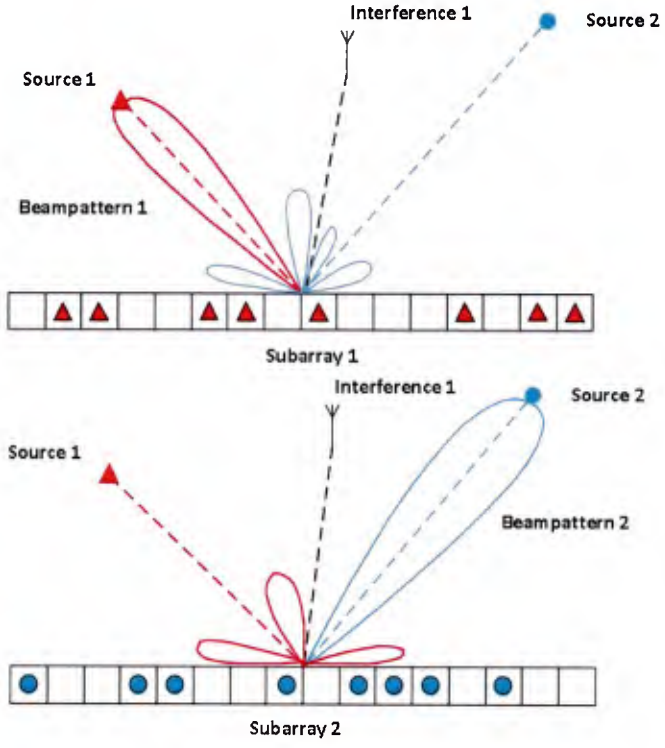

Figure 1: Model of two separated sparse subarrays addressing two sources, one interference

We consider a uniform linear array (ULA), consisting of N isotropic antennas with positions given by $y_n d$, $n = 1, \dots, N$, where d denotes the inter-element spacing. Suppose there are P sources impinging on the array from directions defined by $\{\phi_{s,1}, \dots, \phi_{s,P}\}$. The main goal of this work is to jointly design P sparse, non-overlapping subarrays that collectively span the entire length of the ULA. Depending on the assigned mission, each subarray is tasked either with communicating with a source or detecting the presence of a target along a specified direction. The number of antennas in subarray i is given by K_i, $i = 1, \dots, P$ with coordinates specified by $y_{in} d$, $n = 1, \dots, K_i$. Assume there are m interfering signals impinging on the array from angles $\{\phi_{i,1}, \dots, \phi_{i,m}\}$. For the communications applications, all $P - 1$ emitters other than the one tasked to a given subarray are considered interferences for that subarray. Depending on signal carrier and bandwidth, these interferences can be full-band or partial-band interferences. For a radar function, interference will only be present if target backscatterings are in the same range Doppler cell. An illustrative example of a setup with two sparse non-overlapping subarrays and an interfering source is presented in Fig.1. The receive steering vectors for subarray i towards direction ϕ can be written as:

$$\mathbf{a}_i(\phi) = [e^{jk_0 y_{i1} d\cos\phi}, \dots, e^{jk_0 y_{iK_i} d\cos\phi}]^T, \quad i = 1, \dots, P \tag{1}$$

where k_0 is the wavenumber and is given by $k_0 = 2\pi/\lambda$ with λ denoting the wavelength. The received signals for subarray i at time instant t can be written as:

$$\mathbf{x}_i(t) = s_i(t)\mathbf{a}_i(\phi_{si}) + \mathbf{C}_i\mathbf{c}_i(t) + \mathbf{n}_i(t) \tag{2}$$

where $\mathbf{C}_i = [\mathbf{a}_i(\phi_{s,1}), \dots, \mathbf{a}_i(\phi_{s,i-1}), \mathbf{a}_i(\phi_{s,i+1}), \dots, \mathbf{a}_i(\phi_{s,P}), \mathbf{a}_i(\phi_{i,1}), \dots, \mathbf{a}_i(\phi_{i,m})]$ denotes the interference array manifold matrix with full column rank regarding subarray i, $i = 1, \dots, P$. The source i signal is represented by $s_i(t) \in \mathbb{C}$, $i = 1, \dots, P$, with corresponding power σ_{is}^2. The interfering signals for subarray i are given by the vector $\mathbf{c}_i(t) = [s_1(t), \dots, s_{i-1}(t), s_{i+1}(t), \dots, s_P(t), c_1(t), \dots, c_m(t)] \in \mathbb{C}^{m+P-1}$, with covariance matrix $\mathbf{R}_{bi}$ and $\mathbf{n}_i(t) \in \mathbb{C}^{K_i}$ denotes the received Gaussian noise vector at subarray i. We presume that the noise vectors for all subarrays have common power given by σ_n^2.

The received signal at subarray i is filtered by the receive weight, or coefficient, vector of subarray i denoted as $\mathbf{w}_i \in \mathbb{C}^{K_i}$. Thus, the output SINR for source i is written as

$$\mathrm{SINR}_i = \frac{\sigma_{is}^2 |\mathbf{w}_i^H \mathbf{a}(\phi_{s,i})|^2}{\mathbf{w}_i^H \mathbf{R}_{n,i} \mathbf{w}_i} \tag{3}$$

where $\mathbf{R}_{n,i} = \mathbf{C}_i \mathbf{R}_{b,i} \mathbf{C}_i^H + \sigma_n^2 \mathbf{I}_{K_i}$ defines the interference plus noise covariance matrix for subarray i. The MVDR beamformer that maximizes the SINR, by securing the desired source signal while suppressing the undesired interference and noise, is written as [7]:

$$\mathbf{w}_i = \frac{\mathbf{R}_{n,i}^{-1} \mathbf{a}(\phi_{s,i})}{\mathbf{a}(\phi_{s,i})^H \mathbf{R}_{n,i}^{-1} \mathbf{a}(\phi_{s,i})} \tag{4}$$

By substituting (4) into (3), we obtain the output SINR of the matched MVDR beamformer at subarray i as:

$$\mathrm{SINR}_i = \sigma_{is}^2 \mathbf{G}_i = \sigma_{is}^2 \mathbf{a}(\phi_{s,i})^H \mathbf{R}_{n,i}^{-1} \mathbf{a}(\phi_{s,i}), \tag{5}$$

where

$$\mathbf{G}_i = \mathbf{a}(\phi_{s,i})^H \mathbf{R}_{n,i}^{-1} \mathbf{a}(\phi_{s,i}) \tag{6}$$

denotes the i_{th} subarray gain of the MVDR beamformer towards the direction of source i ($\phi_{s,i}$). It is evident from (1) that the subarray configuration affects the receive steering vectors and hence, from (5), the output SINR for every subarray. To show analytically the full extent of the effect of the subarray selection on the output SINR, we utilize the matrix inversion lemma and restate the interference plus noise covariance matrix $\mathbf{R}_{n,i}^{-1}$ as:

$$\mathbf{R}_{n,i}^{-1} = \sigma_n^2 [\mathbf{I}_{K_i} - \mathbf{C}_i (\mathbf{R}_{m,i} + \mathbf{C}_i^H \mathbf{C}_i)^{-1} \mathbf{C}_i^H] \tag{7}$$

where $\mathbf{R}_{m,i} = \sigma_n^2 \mathbf{R}_{b,i}^{-1}$. By defining $\mathrm{SNR}_i = \sigma_{is}^2 / \sigma_n^2$ as the input signal-to-noise ratio (SNR) at subarray i and substituting (7) into (5), the output SINR at subarray A can be written as in (8). It is evident from (8) that the output SINR of the MVDR beamformer at subarray i is influenced by the subarray configuration through the source steering vectors $\mathbf{a}(\phi_{si})$ and the interference array manifold matrix $\mathbf{C}_i$.

$$\mathrm{SINR}_i = \mathrm{SNR}_i [K_i - \mathbf{a}(\phi_{s,i})^H \mathbf{C}_i (\mathbf{R}_{m,i} + \mathbf{C}_i^H \mathbf{C}_i)^{-1} \mathbf{C}_i^H \mathbf{a}(\phi_{s,i})] \tag{8}$$

3 Sparse Subarray Design through SINR Optimization

3.1 Given Cardinality of Antennas per Subarray

The optimum sparse subarray design can be defined as dividing the full ULA into P separate subarrays that collectively cover the entire ULA and selecting the optimal grid location for each subarray with the respective weights determined by MVDR beamforming. The optimum configuration of the subarrays is obtained by jointly maximizing the SINRs at the output of the different subarrays. In this section, we assume that the number of antennas that constitute each subarray is given, i.e. the values of K_i, $\forall i$ are prefixed and determined a priori. This number can be decided based on the achievable array gain. Hence, the main objective is to simultaneously select the optimum subarray configurations in order to maximize the SINR for each source. Towards that objective, we define P selection vectors $\mathbf{z}_i \in \{0,1\}^N$, $i = 1, \dots, P$, where entry "1" stands for a selected location and "0" for a discarded location for antenna placement regarding subarray i. Since we assume knowledge of all the antenna locations, we may define the full array receive steering vector towards direction ϕ as:

$$\hat{\mathbf{a}}(\phi) = [e^{jk_0 y_1 d\cos\phi}, \dots, e^{jk_0 y_N d\cos\phi}]^T. \tag{9}$$

Therefore, the respective receive steering vectors for subarray i towards angle ϕ can be given by $\mathbf{a}_i(\phi) = \mathbf{z}_i \odot \hat{\mathbf{a}}(\phi)$ and dispose of the zero entries in order to have a vector of length K_i. In order to simultaneously design the optimal sparse, separate subarrays, we consider the following joint output SINR maximization problem:

$$\max_{\mathbf{z}_1,\dots,\mathbf{z}_P} \quad \sum_{i=1}^{P} \mathrm{SINR}_i \tag{10}$$

$$s.t. \quad \mathbf{1}_N^T \mathbf{z}_i = K_i, \forall i$$

$$\sum_{i=1}^{P} \mathbf{z}_i = \mathbf{1}_N$$

$$\mathbf{z}_i \in \{0,1\}^N, \forall i$$

The first constraint in (10) dictates the number of antennas in each subarray. The second and the third constraints ensure that the disjoint subarrays collectively span the entire ULA and that the elements of the selection vectors are strictly 0 or 1, respectively. From (5), the SINR

maximization problem (10) can be restated as a subarray gain optimization problem. In particular, we can define the gain for the full ULA case by substituting (7) into (6) and replacing the subarray steering vectors with the full array steering vectors as shown in (11), where $\hat{\mathbf{C}}_{a,i} = [\hat{\mathbf{C}}_i, \hat{\mathbf{a}}_i(\phi_{s,i})]$ and $\hat{\mathbf{C}}_i$ is defined in (12). The extended interference covariance matrix can be written as:

$$\hat{\mathbf{G}}_i = \sigma_n^2[\hat{\mathbf{a}}(\phi_{s,i})^H\hat{\mathbf{a}}(\phi_{s,i}) - \hat{\mathbf{a}}(\phi_{s,i})^H\hat{\mathbf{C}}_i(\mathbf{R}_{m,i} + \hat{\mathbf{C}}_i^H\hat{\mathbf{C}}_i)^{-1}\hat{\mathbf{C}}_i^H\hat{\mathbf{a}}(\phi_{s,i})] = \sigma_n^2\frac{|\hat{\mathbf{C}}_{a,i}^H\hat{\mathbf{C}}_{a,i}+\mathbf{R}_i|}{|\hat{\mathbf{C}}_i^H\hat{\mathbf{C}}_i+\mathbf{R}_{m,i}|} \quad (11)$$

$$\hat{\mathbf{C}}_i = [\hat{\mathbf{a}}_i(\phi_{s,1}), \dots, \hat{\mathbf{a}}_i(\phi_{s,i-1}), \hat{\mathbf{a}}_i(\phi_{s,i+1}), \dots, \hat{\mathbf{a}}_i(\phi_{s,P}), \hat{\mathbf{a}}_i(\phi_{i,1}), \dots, \hat{\mathbf{a}}_i(\phi_{i,m})] \quad (12)$$

$$\mathbf{R}_i = \begin{bmatrix} \mathbf{R}_{m,i} & \mathbf{0}_{1\times m} \\ \mathbf{0}_{m\times 1} & 0 \end{bmatrix}.$$

The equality in (11) can be proved by utilizing the block matrix determinant formula, as shown below:

$$|\hat{\mathbf{C}}_{a,i}^H\hat{\mathbf{C}}_{a,i} + \mathbf{R}_i| = \begin{vmatrix} \hat{\mathbf{C}}_i^H\hat{\mathbf{C}}_i + \mathbf{R}_{m,i} & \hat{\mathbf{C}}_i^H\hat{\mathbf{a}}(\phi_{s,i}) \\ \hat{\mathbf{a}}(\phi_{s,i})^H\hat{\mathbf{C}}_i & \hat{\mathbf{a}}(\phi_{s,i})^H\hat{\mathbf{a}}(\phi_{s,i})^H \end{vmatrix}$$

$$= |\hat{\mathbf{C}}_i^H\hat{\mathbf{C}}_i + \mathbf{R}_{m,i}|\hat{\mathbf{G}}_i. \quad (13)$$

Hence, the SINR maximization (10) can be reformulated as the maximization of the logarithm of the subarray gain for each subarray as [36],

$$\max_{\mathbf{z}_1,\dots,\mathbf{z}_P} \sum_{i=1}^P \log|\hat{\mathbf{C}}_{a,i}^H\mathcal{D}(\mathbf{z}_i)\hat{\mathbf{C}}_{a,i} + \mathbf{R}_i| - \log|\hat{\mathbf{C}}_i^H\mathcal{D}(\mathbf{z}_i)\hat{\mathbf{C}}_i + \mathbf{R}_{m,i}|$$

$$s.t. \quad \mathbf{1}_N^T\mathbf{z}_i = K_i, \forall i \quad (14)$$

$$\sum_{i=1}^P \mathbf{z}_i = \mathbf{1}_N$$

$$\mathbf{z}_i \in \{0,1\}^N, \forall i$$

where $\mathcal{D}(\mathbf{z}_i)$ denotes the diagonal matrix populated with the vector $\mathbf{z}_i$ along the diagonal. There are two reasons that render the optimization (14) non-convex: the non-concave objective function, that is defined as the difference of concave functions, and the non-convex binary constraint enforced by the antenna selection vectors $\mathbf{z}_i \in \{0,1\}^N$. However, since the objective

function is the difference of concave functions, the respective global optimizer locates at the extreme points of the polyhedron and thus we may replace the binary constraint with the box constraint $0 \leq \mathbf{z}_i \leq 1$ [17, 33]. To circumvent the non-concavity of the objective function, we utilize first order Taylor series that can iteratively approximate the negative logarithms of the objective function, which cause the non-concavity. The $(k+1)_{th}$ Taylor approximations of those terms based on the previous solution $\mathbf{z}_i^{(k)}$ are shown in (15), where $\nabla \mathbf{g}_i(\mathbf{z}_i^{(k)})$ represents the gradient of the logarithmic function $\log|\hat{\mathbf{C}}_i^H \mathcal{D}(\mathbf{z}_i)\hat{\mathbf{C}}_i + \mathbf{R}_{m,i}|$ evaluated at the point $\mathbf{z}_i^{(k)}$ and is written as in (16), where $\hat{\mathbf{a}}_{i,j}$ denotes the j_{th} column vector of the matrix $\hat{\mathbf{C}}_i^H$. This sequential convex programming (SCP) technique recasts the initially non-convex problem to a series of convex subproblems, each

$$\log|\hat{\mathbf{C}}_i^H \mathcal{D}(\mathbf{z}_i)\hat{\mathbf{C}}_i + \mathbf{R}_{m,i}| \approx \log|\hat{\mathbf{C}}_i^H \mathcal{D}(\mathbf{z}_i^k)\hat{\mathbf{C}}_i + \mathbf{R}_{m,i}| + \nabla \mathbf{g}_A^T(\mathbf{z}_i^{(k)})(\mathbf{z}_i - \mathbf{z}_i^{(k)}) \triangleq T_i \quad (15)$$

$$\nabla \mathbf{g}_i(\mathbf{z}_i^{(k)}) = [\hat{\mathbf{a}}_{i,j}^H (\hat{\mathbf{C}}_i^H \mathcal{D}(\mathbf{z}_i^{(k)})\hat{\mathbf{C}}_i + \mathbf{R}_{m,i})^{-1} \hat{\mathbf{a}}_{i,j}, j = 1, \ldots, N]^T \quad (16)$$

of which can be optimally solved via convex optimization [4]. By substituting (15) into (14), we obtain the following approximated convex optimization problem that provides the antenna selection in the $(k+1)_{th}$ iteration based on the solution $\mathbf{z}_i^{(k)}$, $\forall i$ from the previous iteration:

$$\begin{aligned} \max_{\mathbf{z}_1, \ldots, \mathbf{z}_P} \quad & \sum_{i=1}^{P} \log|\hat{\mathbf{C}}_{a,i}^H \mathcal{D}(\mathbf{z}_i)\hat{\mathbf{C}}_{a,i} + \mathbf{R}_i| - T_i \\ s.t. \quad & \mathbf{1}_N^T \mathbf{z}_i = K_i, \forall i \\ & \sum_{i=1}^{P} \mathbf{z}_i = \mathbf{1}_N \\ & 0 \leq \mathbf{z_i} \leq 1, \forall i \end{aligned} \quad (17)$$

It should be highlighted that SCP is a local heuristic and thus the final solution is dependent on the initial subarray selection vectors $\mathbf{z}_i^{(0)}$, $\forall i$. Hence, we consider several initialization points $\mathbf{z}_i^{(0)}$, $\forall i$ for optimization (17) and select the solution that provides the maximum objective function value. We use the Matlab embedded CVX software [14] to solve problem (17).

3.2 Cardinality as an Optimization Variable

In this subsection, we consider the cardinality of the antennas in each subarray as an optimization variable of the SINR maximization problem (17). Adding the numbers of sensors per subarray as an optimization variable maintains the convexity of the SCP optimization problem (17) and the reformulated problem can be written as:

$$\max_{\substack{\mathbf{z}_1,\ldots,\mathbf{z}_P \\ K_1,\ldots,K_P}} \quad \sum_{i=1}^{P} \log|\hat{\mathbf{C}}_{a,i}^H \mathcal{D}(\mathbf{z}_i)\hat{\mathbf{C}}_{a,i} + \mathbf{R}_i| - T_i$$

$$s.t. \quad \mathbf{1}_N^T \mathbf{z}_i = K_i, \forall i \tag{18}$$

$$\sum_{i=1}^{P} \mathbf{z}_i = \mathbf{1}_N$$

$$0 \leq \mathbf{z_i} \leq 1, \forall i$$

In this case, the optimization does not only decide the location of the sparse subarrays sensors but also their number, i.e. K_i, $i = 1, \ldots, P$, based on the mission information and requirements. It should be highlighted that this method should be applied in cases where there is no minimum requirement regarding the performance of the system for each source, since the solution will allocate more antennas to a source with higher channel gain.

4 Optimum Subarray Design through SINR Constrained Optimization

The common aperture dual or multitask receiver platforms must provide a sufficient gain to the incoming signal regardless of whether it represents communication or radar data. This gain improves successful decoding of symbols for the former case and enhances probability of target detection for the latter case. Hence, in this section our primary objective is to design an algorithm that maximizes the SINR for some sources subject to attaining a specific set of SINRs for the remaining sources. By setting the cardinality of the antennas as an optimization variable, the proposed scheme not only derives the optimum sparse subarray configurations but also the optimal number of antennas (K_i, $\forall i$) for each subarray.

Without loss of generality, we consider that there is a predefined SINR criterion γ_l^*, $l = 1, \ldots, L$ for the first L out of a total of P sources of interest. With a total of N antennas placed on a uniform linear grid, we may define the optimum sparse subarray design with SINR constraints

as selecting the optimum sparse subarrays that constitute a ULA. Each subarray considers one source of interest and jointly maximizes the SINR_i performance towards $P-L$ sources where $i=L+1,\ldots,P$, while attaining the SINR threshold γ_l^*, $l=1,\ldots,L$ for the rest of the sources. To achieve this arrangement, we consider the following constrained-SINR maximization problem:

$$\max_{\substack{\mathbf{z}_1,\ldots,\mathbf{z}_P \\ K_1,\ldots,K_P}} \quad \sum_{i=L+1}^{P} \mathrm{SINR}_i \tag{19}$$

$$s.t. \quad \mathrm{SINR}_l \geq \gamma_l^*, l=1,\ldots,L$$

$$\mathbf{1}_N^T \mathbf{z_i} = K_i, \forall i$$

$$\sum_{i=1}^{P} \mathbf{z}_i = \mathbf{1}_N$$

$$\mathbf{z}_i \in \{0,1\}^N, \forall i$$

The non-concave objective function and SINR constraints and also the non-convex binary selection constraints $\mathbf{z}_i \in \{0,1\}^N$ render the optimization (19) non-convex. Similarly to section III, we relax the selection vector constraints to box constraints and we exploit first order Taylor series approximation SCP to iteratively approximate the objective function and the SINR constraints. We derive the following approximated convex optimization problem:

$$\max_{\substack{\mathbf{z}_1,\ldots,\mathbf{z}_P \\ K_1,\ldots,K_P}} \quad \sum_{i=L+1}^{P} \log|\hat{\mathbf{C}}_{a,i}^H \mathcal{D}(\mathbf{z}_i)\hat{\mathbf{C}}_{a,i} + \mathbf{R}_i| - T_i$$

$$s.t. \quad \log|\hat{\mathbf{C}}_{a,l}^H \mathcal{D}(\mathbf{z}_l)\hat{\mathbf{C}}_{a,l} + \mathbf{R}_l| - T_l \geq \gamma_l^*, l=1,\ldots,L$$

$$\mathbf{1}_N^T \mathbf{z}_i = K_i, \forall i \tag{20}$$

$$\sum_{i=1}^{P} \mathbf{z}_i = \mathbf{1}_N$$

$$0 \leq \mathbf{z_i} \leq 1, \forall i$$

The optimization (20) is a local heuristic problem and its solution depends on the initialization vectors $\mathbf{z}_i^{(0)}$. Hence, we initialize the SCP algorithm (20) with several starting points $\mathbf{z}_i^{(0)}$ and save the solution that gives the maximum objective function value.

5 Simulation Results

In this section, simulation results are presented to validate the effectiveness of the proposed joint aperture optimum subarray design algorithms.

5.1 Example 1

We consider a ULA consisting of $N = 16$ antennas with an inter-element spacing of $d = \lambda 2$. The receiving platform aims to maximize the SINR of two separate sources utilizing two sparse subarrays of fixed number of antennas, $K_1 = K_2 = 8$. The first source signal arrives at the array from a direction $\phi_{s,1}$ that is changing from 0^o to 180^o with a step of 3^o, and with an SNR set at 0dB, whereas the second source is fixed at $\phi_{s,2} = 45^o$, with an SNR of 3dB. An interfering source is also active, impinging on the ULA from $\phi_{i,1} = 112^o$ with an INR set at 20dB. For each arrival angle of source 1, we obtain the corresponding optimum sparse subarrays regarding both sources according to SINR maximization (17), and using 12 random initialization points $\mathbf{z}_i^{(0)}$. In order to validate the efficiency of the first order Taylor series approximation SCP, we obtain the true optimum sparse subarrays through enumeration and compare the output SINRs of both methods in Fig.2. It is evident that the optimum performance of the proposed method closely approximates the global optimum solution obtained from enumeration. Moreover, there is an evident SINR drop for both subarrays when the two sources are closely separated, since each source, in essence, plays the role of an interfering signal for the reception of the other source. Subarray 1 experiences one more SINR drop when source 1 is closely located to the interfering source, whereas this drop is not present for subarray 2, since source 2 is fixed at $\phi_{s,2} = 45^o$. In order to demonstrate the impact of the subarray configuration on the output SINR, we fix the incoming angle of source 1 at $\phi_{s,1} = 143^o$ and enumerate all possible 12870 subarray selections. We present the corresponding output SINR in descending values for both sources in Fig.3. The cardinalities of all possible selections for subarrays 1 and 2 are obtained from $\frac{N!}{K_1!\,(N-K_1)!}$ and $\frac{N!}{K_2!\,(N-K_2)!}$, respectively, which are equal, since $N = K_1 + K_2$. It is clear that the different subarray designs significantly alters the output SINR, up to 5dB difference. As mentioned in section III, the number of initialization points $\mathbf{z}_i^{(0)}$ affects the performance of the optimization (17). Table 1 presents the output SINR for subarrays 1 and 2 for different number of initialization vectors $\mathbf{z}_i^{(0)}$. It is evident that there is a minor increase in performance with increased number of initialization

points. It also shows that even by using few initialization points, we achieve a performance that closely approximates the global optimum, which is $\text{SINR}_1^* = 9.0306$ and $\text{SINR}_2^* = 12.0302$. Simulations also showed that there is insignificant change in SINR when using more than 12 initialization points. [1]

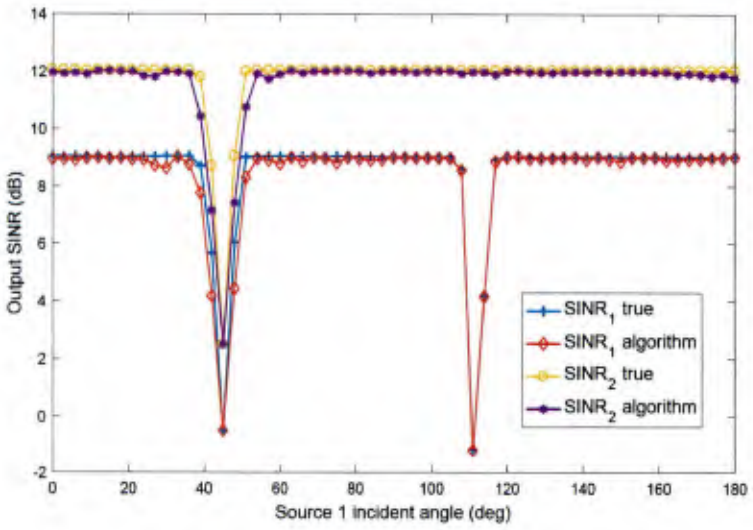

Figure 2: Output SINR for subarrays 1 and 2 derived from enumeration and (17).

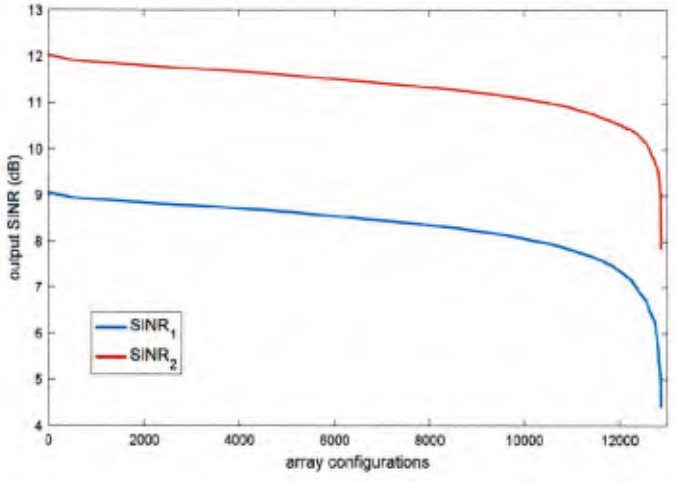

Figure 3: Output SINR for all different sparse subarrays for ϕ_(s,1)=143^o and ϕ_(s,2)=45^0.

[1] Regarding the computational complexity of the proposed algorithm, it is noted that the complexity of an $N \times N$ matrix inversion is of the order $O(N^3)$ and the solution of a convex problem is of polynomial time complexity. In the proposed algorithm, we perform $m_{iter} \times n_{iter}$ iterations, where m_{iter} is the number of initialization points of the respective optimization and n_{iter} is the number of iterations needed to achieve the required Taylor approximation accuracy. During each iteration, P matrix inversions and P convex optimizations are performed, where P is the number of desired sources considered.

Table 1: Maximum SINR for (17) with varying number of initialization points $\mathbf{z}_i^{(0)}$ (dB).

Number of $\mathbf{z}_i^{(0)}$	$SINR_1$	$SINR_2$
2	8.9851	11.9685
4	8.9851	11.9728
6	8.9928	11.9728
8	9.0024	12.0134
10	9.0118	12.0188
12	9.0216	12.0242
14	9.0216	12.0242
16	9.0216	12.0242

5.2 Example 2

In the next simulation, we extend the ULA to $N = 36$ antennas and add a third source of interest at $\phi_{s,3} = 68^o$ with SNR fixed for all sources at 0dB. The interfering source is assumed to be the same as in the first example. We assume two cases of highly and weakly spatially correlated sources. Case I represents highly spatially correlated sources, where the incident angles of sources 1 and 2 are set at $\phi_{s,1} = 47^o$ and $\phi_{s,2} = 45^o$, respectively. In case II of low spatial correlation, the angles-of-arrival are set at $\phi_{s,1} = 143^o$ and $\phi_{s,2} = 45^o$, respectively. The spatial correlation matrices of the steering vectors corresponding to sources 1 and 2 for the high and the low correlation cases are:

$$\mathbf{R}_{high} = \begin{bmatrix} 1 + 0j & 0.1318 + 0.6837j \\ 0.1318 - 0.6837j & 1 + 0j \end{bmatrix},$$

$$\mathbf{R}_{low} = \begin{bmatrix} 1 + 0j & 0.0060 + 0.0118j \\ 0.0060 - 0.0118j & 1 + 0j \end{bmatrix}.$$

In order to shed light on the mechanism of joint subarray design, we derive the optimum subarrays for the two cases of given antennas cardinality and when the cardinality is a design parameter which are associated with (17) and (18), respectively. We also obtain the optimal subarrays by maximizing the output SINR for each of the sources when considered separately through the following optimization:

$$\max_{\mathbf{z}} \quad \text{SINR}_{oi} \tag{21}$$

$$s.t. \quad \mathbf{1}_N^T \mathbf{z} = K$$

$$0 \leq \mathbf{z} \leq 1$$

for $i = 1, \ldots, P$. Optimization (21) is non-convex and can be recasted as a convex one by using SCP. Since there is no explicit constraint on shared antennas across subarrays, some antennas could be allocated to more than one subarray and hence this design cannot be used for simultaneous multitask function. The subarray configurations derived from (17), (18) and (21) are depicted in Figs. 4 and 5 for the highly and the weakly correlated cases, respectively. In particular, the blue dots represent the respective active sensors for the corresponding subarray. Two important observations are in order: Firstly, for the case of highly spatially correlated sources, the optimum subarrays for sources 1 and 2 obtained from the separate design (21) are fully overlapped (Fig.4 (g),(h)), since they consist of exactly the same antennas, whereas for the weakly correlated case they share only 4 out of 12 antennas (Fig.5 (d),(e)). Hence, the competition for the optimum antennas located at the two far edges of the ULA in the joint aperture subarray design is more intense for higher spatial correlation of the sources of interest. As depicted in Fig.4, subarrays 1 and 2 from (17) and (18) contest over the optimal antennas located at the two far edges of the ULA, whereas most of the antennas in the center of the ULA are allocated to subarray 3. The second observation is that the optimum subarray configurations from both (17) and (18) is exactly the same for the weakly correlated sources, as seen in Fig.5. However, for the case of highly correlated sources, optimization (18) allocates more antennas to the less correlated source 3 ($K_1 = 10$, $K_2 = 11$, $K_3 = 15$), since it results in higher total SINR for the system, as shown in Table 2. This table presents the maximum output SINR values and the total SINR for all three sources for optimizations (17), (18) and (21). It is also evident from Table 2 that for the case of highly correlated sources, the proposed methods provide a substantially lower SINR as compared to

separate subarray optimization. On the other hand, for less correlated sources the joint optimizations (17) and (18) provide almost identical performance to the separate design technique (21). The beampatterns for the optimum subarrays obtained from (17) for the highly and weakly correlated cases are plotted in Figs.6 and 7, respectively.

Figure 4: Arrays for case I: (a) Subarray 1 for given cardinality of antennas (17), (b) Subarray 2 from (17), (c) Subarray 3 from (17), (d) Subarray 1 when the cardinality is a design parameter (18), (e) Subarray 2 from (18), (f) Subarray 3 from (18), (g) Subarray 1 from separate design (21), (h) Subarray 2 from (21), (i) Subarray 3 from (21).

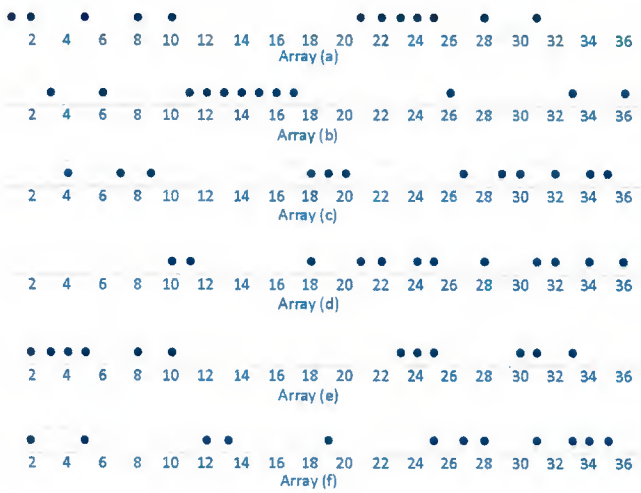

Figure 5: Arrays for case II: (a) Subarray 1 for given cardinality of antennas (17) and when the

cardinality is a design parameter (18), (b) Subarray 2 from (17) and (18), (c) Subarray 3 from (17) and (18), (d) Subarray 1 from (21), (e) Subarray 2 from (21), (f) Subarray 3 from (21).

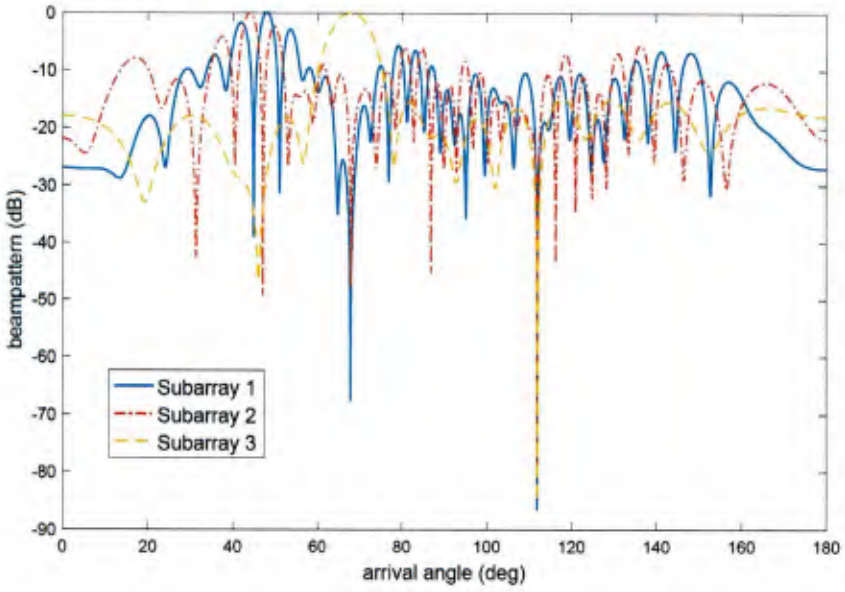

Figure 6: The beampatterns for all subarrays for case I from (17).

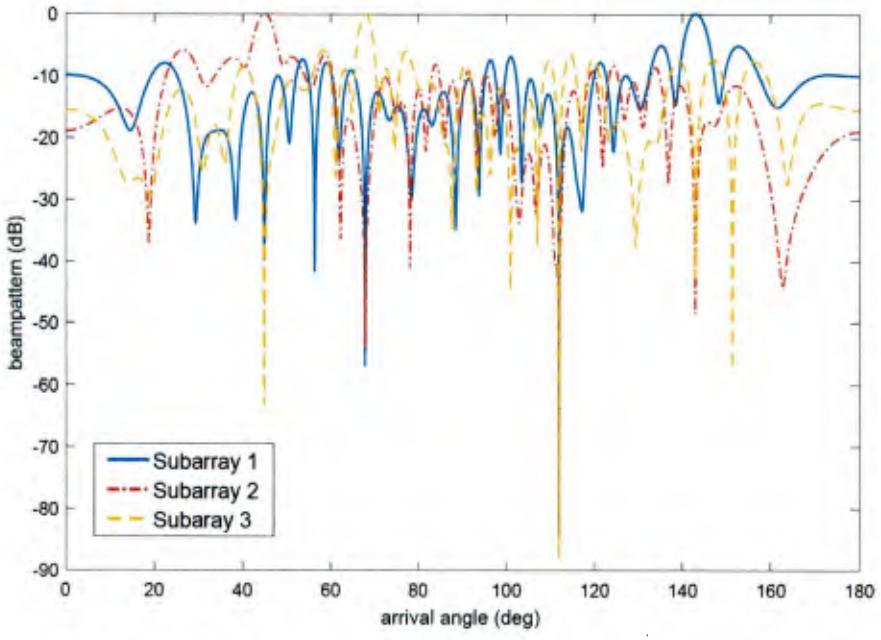

Figure 7: The beampatterns for all subarrays for case II from (17).

Table 2: Maximum SINR for the proposed methods of (17), (18) and separate optimization (21) (dB).

	Eq.(17)	Eq.(18)	Eq.(21)
$SINR_1$, Case I	9.1294	8.5465	10.1743
$SINR_2$, Case I	9.1989	9.2434	10.1698
$SINR_3$, Case I	10.7389	11.7027	10.7529
Total SINR, Case I	29.0672	29.4926	31.097
$SINR_1$, Case II	10.7434	10.7434	10.7435
$SINR_2$, Case II	10.6530	10.6530	10.7537
$SINR_3$, Case II	10.6844	10.6844	10.7547
Total SINR, Case II	32.0808	32.0808	32.2519

5.3 Example 3

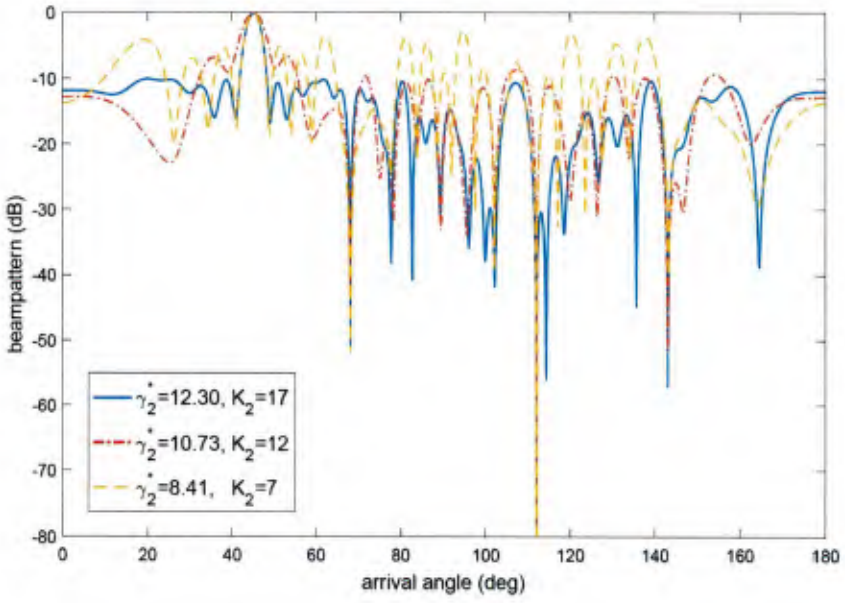

Figure 8: Beampatterns towards source 2 for different γ_2^*.

Table 3: Optimal number of antennas for subarays 1, 2 and 3 and maximum $SINR_1$ and $SINR_3$ (dB) for different target SINR γ_2^*.

$SINR_2$ target	K_1	K_2	K_3	$SINR_1$	$SINR_3$
$\gamma_2^* = 8.41$	14	7	15	11.38	11.73
$\gamma_2^* = 10.73$	12	12	12	10.77	10.75
$\gamma_2^* = 12.30$	10	17	9	9.88	9.45

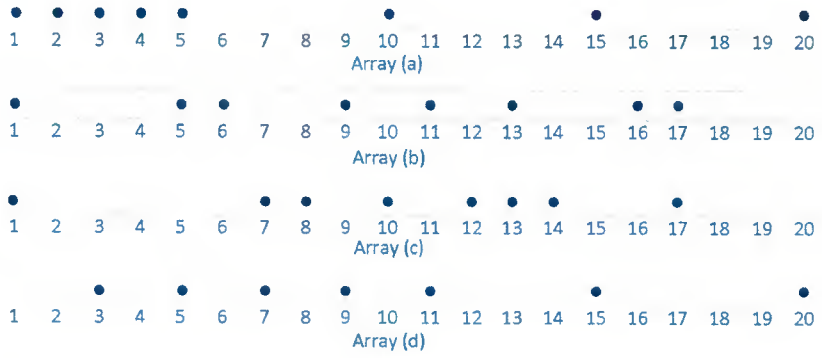

Figure 9: Subarray 1: (a) proposed method (17), (b) Nested array, (c) Coprime array, (d) proposed method (20) with $\gamma_1^* = 8.4102$.

In this simulation, we consider the same layout as the weak correlation case of the previous example. We assume a predefined fixed desired SINR_2 for source 2. The primary objective is to obtain three separate sparse subarrays that constitute the entire ULA and maximize the SINR at the output of subarrays 1 and 3 while satisfying the desired output SINR for subarray 2. It is noted that the algorithm decides on both the optimal locations of the antennas for each subarray and also the optimal number of antennas for each subarray (K_1, K_2, K_3). The beampatterns towards source 2 for different SINR thresholds γ_2^* are shown in Fig.8. It is evident that higher γ_2^* generates a more accurate mainbeam towards source 2 with lower sidelobe levels and more efficient mitigation of interference. The optimum cardinality of the antennas in each subarray along with the maximum SINRs obtained from (20) for different γ_2^* are listed in Table 3. As expected, the higher the desired SINR level towards source 2 is, the more antennas are allocated to subarray 2, which

naturally leads to a drop of SINR for the other subarrays.

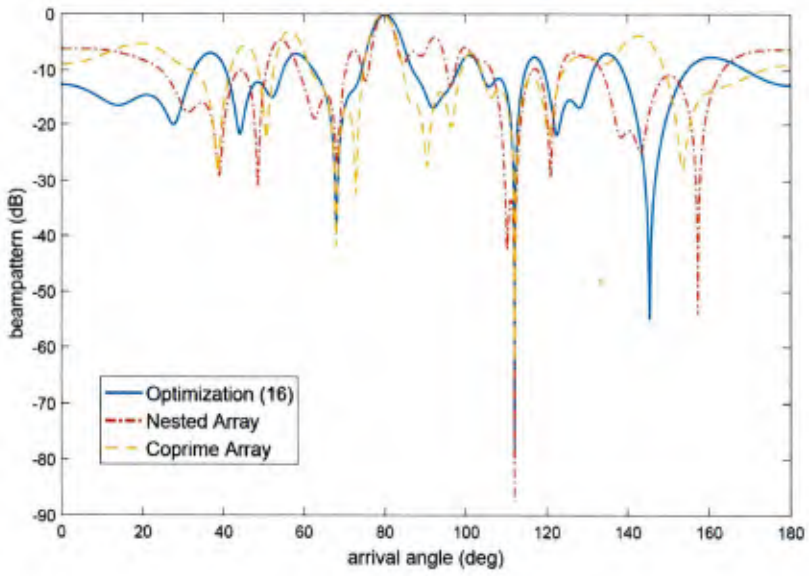

Figure 10: Beampatterns for subarrays (a), (b) and (c) in Fig.9.

Table 4: Comparison of the system performance for the proposed methods, the nested arrays and the coprime arrays schemes.

	K_1	K_2	$SINR_1$	$SINR_2$
Optimization (17)	8	12	8.9639	13.7877
Nested	8	12	8.4102	13.3058
Coprime	8	12	7.9412	13.4557
Optimization (20), $\gamma_1^* = 8.4102$	7	13	8.4102	14.1116

5.4 Example 4

In order to further demonstrate the superiority of the proposed adaptive algorithms, we compare the performance of the sparse subarrays obtained from (17) to the case when the structured nested and coprime arrays are utilized to derive subarray 1 [1, 27]. We consider a ULA of $N = 20$ antennas and two sources of interest. For a fair comparison, we employ $K_1 = 8$ antennas to design the optimum adaptive sparse subarray 1 from (17) and also 8 antennas to build the prefixed nested and coprime subarray 1. The angles-of-arrival of the sources of interest are $\phi_{s,1} = 80^o$ and $\phi_{s,2} = 68^o$ with their SNR set at 0dB. An interfering source is also present at $\phi_{i,1} = 112^o$ with INR $= 20dB$. The subarray 1 structures are depicted in Fig.9 and the corresponding beampatterns in Fig.10. It can be observed that the proposed joint sparse subarray design yields a better shaped beampattern with deeper nulls at the direction of interference and lower sidelobes when contrasted with the prefixed nested and coprime arrays beampattern. In order to quantify the comparison, Table 4 shows the maximum SINR obtained from the proposed adaptive algorithms and the prefixed techniques. We also added the optimum subarray structure obtained from (20) with $\gamma_1^* = 8.4102$ (subarray (d) in Fig.9) to match the SINR performance of the prefixed nested array technique. It is evident that the proposed adaptive algorithms substantially outperform the prefixed nested and coprime schemes in terms of output SINR for the sources of interest. Furthermore, as shown in Table 4, the proposed adaptive optimization (20) matches the performance of the nested arrays structure towards source 1, even though employing only 7 antennas. Therefore, the extra antenna can be allocated to subarray 2, maximizing the SINR_2 performance for source 2 as shown in Table 4.

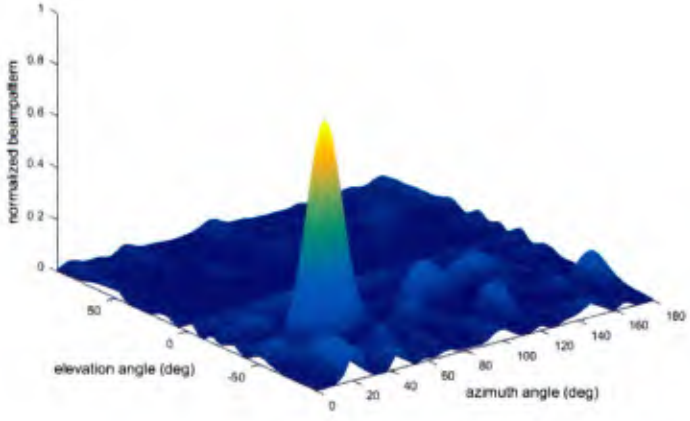

Figure 11: Normalized beampattern of subarray 1.

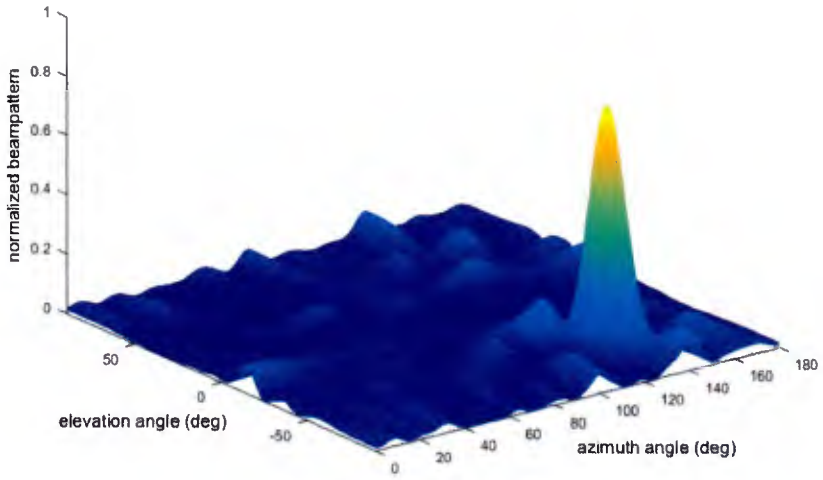

Figure 12: Normalized beampattern of subarray 2.

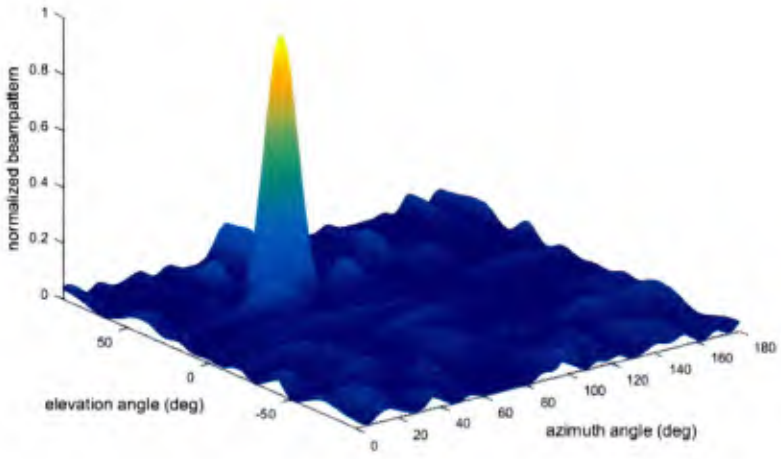

Figure 13: Normalized beampattern of subarray 3.

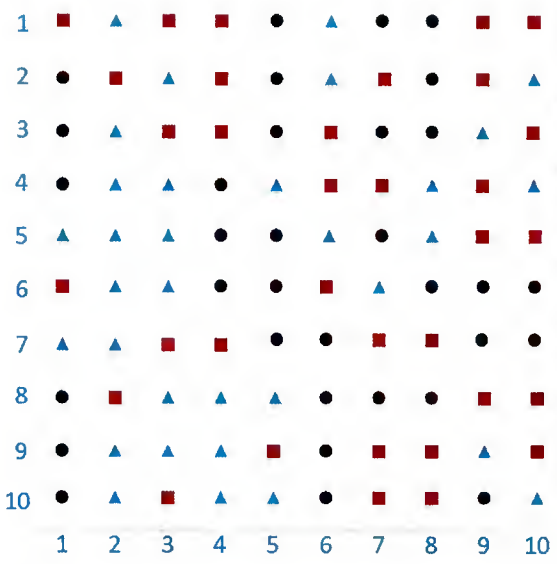

Figure 14: Sparse subarrays configuration map: circle: subarray 1, triangle: subarray 2, square: subarray 3.

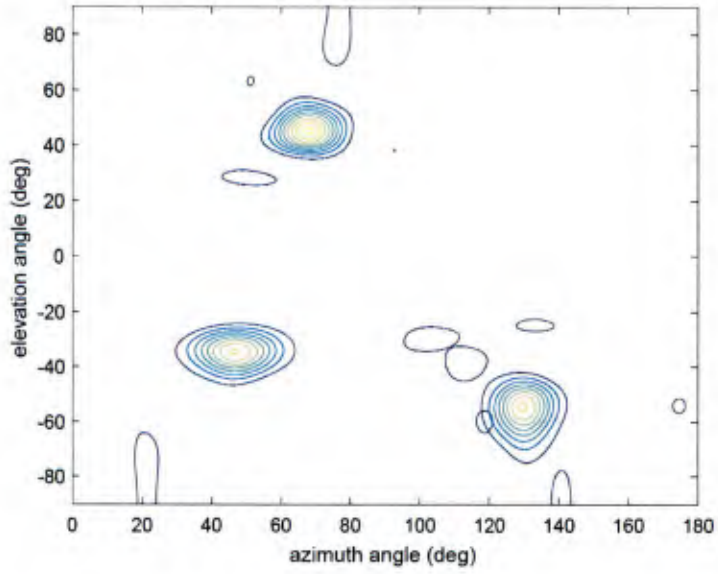

Figure 15: Collective contour plot of the three beampatterns.

5.5 Example 5

The proposed sparse subarray design algorithms can be also applied in the case of planar antenna arrays. For illustration, we consider a 10×10 uniform rectangular array (URA) with an

interelement spacing among any two adjacent antennas along any column or row is $d_x = d_y = \lambda 2$, respectively. Three sources of interest are considered with angles of arrival $\theta_{s,1} = -35^o$, $\theta_{s,2} = -55^o$, $\theta_{s,3} = 45^o$, where $\theta_{s,i}$ denotes the elevation angle of source i and $\hat{\phi}_{s,1} = 47^o$, $\hat{\phi}_{s,2} = 130^o$, $\hat{\phi}_{s,3} = 68^o$, with $\hat{\phi}_{s,i}$ stands for the azimuth angle of source i. There is also one interfering source present impinging on the 2D array from $\theta_{i,1} = 74^o$ (elevation), $\hat{\phi}_{i,1} = 112^o$ (azimuth). We allocate 34 antennas for subarray 3 and 33 antennas for each of the subarrays 1 and 2, i.e. $K_3 = 34$, $K_1 = K_2 = 33$. The respective normalized beampatterns for each subarray are plotted in Figs. 11, 12 and 13. The sparse separated subarrays configuration is shown in Fig.14 and the collective contour plot of all three beampatterns is depicted in Fig.15.

6 Conclusion

We have examined the problem of sparse array design, where the array aperture is divided among different subarrays - a concept known as shared aperture. At first, we proposed an algorithm that optimally decides the locations of predetermined number of antennas for each subarray using SINR as a criterion and conditioned of having unshared antennas among the subarrays. Furthermore, we generalized the above problem by including the cardinality of the antennas in each subarray as an optimization variable, providing more degrees of freedom to the algorithm to further increase the efficiency of the system. Additionally, we proposed an algorithm that maximizes the SINR for some sources, while satisfying a certain SINR threshold for the other sources. Sequential convex programming and Taylor series approximation techniques were employed to render the initially non-convex sparse subarray design as a convex problem. Simulation results demonstrated that the proposed method closely approximates the true optimum sparse subarray design performance obtained by enumeration. Furthermore, it was shown that the proposed algorithm can be applied to high spatially correlated sources and in the case of planar antenna arrays. Finally, the superior performance of the resulting subarrays over other prefixed sparse array configurations was also demonstrated.

References

[1] M> G. Amin, P P Vaidyanathan, Y D Zhang, and Piya Pal. Special issue on coprime sampling and arrays. *Digital Signal Processing*, 61:1–96, 2017.

[2] M. G. Amin, X. Wang, Y. D. Zhang, F. Ahmad, and E. Aboutanios, "Sparse arrays and sampling for interference mitigation and DOA estimation in GNSS," *Proceedings of the IEEE*, 104(6):1302–1317, 2016.

[3] S Applebaum, "Adaptive arrays," *IEEE Transactions on Antennas and Propagation*, 24(5):585–598, 1976.

[4] S. Boyd and L. Vandenberghe. *Convex optimization*. Cambridge University Press, 2004, 2004.

[5] L E Brennan and L S Reed, "Theory of adaptive radar," *IEEE Transactions on Aerospace and Electronic Systems*, AES-9:237–252, 1973.

[6] K. Buckley and L. Griffiths, "An adaptive generalized sidelobe canceller with derivative constraints," *EEE Transactions on Antennas and Propagation*, 34(3):311–319, 1986.

[7] J Capon, "High-resolution frequency-wavenumber spectrum analysis, "*Proceedings of the IEEE*, 57:1408–1418, 1969.

[8] R Compton, "An adaptive array in a spread-spectrum communication system," *Proeedings of the IEEE*, 66(3):289–298, 1978.

[9] A. Deligiannis, S. Lambotharan, and J. A Chambers, "Game Theoretic Analysis for MIMO Radars With Multiple Targets," *IEEE Transactions on Aerospace and Electronic Systems*, 52(6):2760–2774, 2016.

[10] A. Deligiannis, S. Lambotharan, and J. A Chambers, "Beamforming for fully-overlapped two-dimensional Phased-MIMO radar," *IEEE Radar Conference (RadarCon), Arlington, VA, USA, 2015*.

[11] A. Deligiannis, A. Panoui, S. Lambotharan, and J.A. Chambers, "Game-Theoretic Power Allocation and the Nash Equilibrium Analysis for a Multistatic MIMO Radar Network," *IEEE Transactions on Signal Processing*, 65(24):6397–6408, 2017.

[12] O T Demir and T E Tuncer, "Optimum discrete transmit beamformer design," *Digital Signal Processing*, 36:57–68, 2015.

[13] P. E. Dewdney, P. J. Hall, R. T. Schilizzi, and T. J. L. W. Lazio, "The square kilometre array," *Proceedings of the IEEE*, 97(8):1482–1496, 2009.

[14] M. Grant, S. Boyd, and Y. Ye. *CVX: Matlab software for disciplined convex*

programming. 2008.

[15] A. Hassanien, M. W. Morency, A. Khabbazibasmenj, S. A. Vorobyov, J.-Y. Park, and S.-J. Kim. Two-dimensional transmit beamforming for MIMO radar with sparse symmetric arrays. *IEEE Radar Conference (RADAR)*, 2013.

[16] R. L Haupt, "Phase-Only Adaptive Nulling with a Genetic Algorithm, "*IEEE Transactions on Antennas and Propagation*, 45(6):1009–1015, 1997.

[17] R Horst. *Introduction to global optimization*. Springer, 2000.

[18] D. H. Johnson and S. R. Degraaf, "Improving the resolution of bearing in passive sonar arrays by eigenvalue analysis," *IEEE Transactions on Acoustics, Speech, and Signal Processing*, 30(4):638–647, 1982.

[19] S. M Kay. *Fundamentals of Statistical Signal Processing: Detection Theory*. Prentice-Hall, New Jersey, 1998.

[20] G. Kwon, J. Park, D. Kim, and K. C. Hwang, "Optimization of a Shared-Aperture Dual-Band Transmitting/Receiving Array Antenna for Radar Applications, "*IEEE Transactions on Antennas and Propagation*, XX(X):1–14, 2017.

[21] I E Lager, C Trampuz, M Simeoni, C I Coman, and L P Ligthart, "Application of the shared aperture antenna concept to radar front-ends : advantages and limitations, "*Proceedings of the Fourth European Conference on Antennas and Propagation (EuCAP)*, 2010.

[22] H. Lin, "Spatial Correlations in Adaptive Arrays, *IEEE Transactions on Antennas and Propagation*, 30(2):212–223, 1982.

[23] O. Mehanna, N Sidiropoulos, and G Giannakis, " Joint multicast beamforming and antenna selection, "*IEEE Transactions on Signal Processing*, 61(10):2660–2674, 2013.

[24] A F Morabito, A R Lagana, G Sorbello, and T Isernia, "Mask-constrained power synthesis of maximally sparse linear arrays through a compressive-sensing-driven strategy," *Journal of Electromagnetic Waves and Applications*, 29(10):1384–1396, 2015.

[25] P.J. Napier, A.R. Thompson, and R.D. Ekers, "The very large array: Design and performance of a modern synthesize radio telescope," *Proceedings of the IEEE*, 71(11):1295–1320, 1983.

[26] G. Oliveri, F. Viani, and A. Massa, "Synthesis of linear multi-beam arrays through hierarchical almost difference set-based interleaving," *IET Microwaves, Antennas & Propagation*, 8(10):794–808, 2014.

[27] P. Pal and P P Vaidyanathan, "Nested arrays: A novel approach to array processing with enhanced degrees of freedom," *IEEE Trans. on Signal Processing*, 58(8):4167–4181, 2010.

[28] L. Poli, P. Rocca, M. Salucci, and A. Massa, "Reconfigurable thinning for the adaptive control of linear arrays, *IEEE Transactions on Antennas and Propagation*, 61(10):5068–5077, 2013.

[29] D. M. Pozar and S. D. Targonski, "A shared-aperture dual-band dual-polarized microstrip array," *IEEE Transactions on Antennas and Propagation*, 49(2):150–157, 2001.

[30] F. Rashid-farrokhi, K J Ray Liu, and L. Tassiulas, "Transmit Beamforming and Power Control for Cellular Wireless Systems," *IEEE Journal on Selected Areas in Comms.*, 16(8):1437–1450, 1998.

[31] X. Shen and P.K. Varshney, "Sensor selection based on generalized information gain for target tracking in large sensor networks, " *IEEE Transactions on Signal Processing*, 62(2):363–375, 2014.

[32] G. C. Tavik, C. L. Hilterbrick, J. B. Evins, J. J. Alter, J. G. Crnkovich, J. W. De Graaf, W. Habicht, G. P. Hrin, S. A. Lessin, C. Wu, and S. M. Hagewood, "The advanced multifunction RF concept, "*IEEE Transactions on Microwave Theory and Techniques*, 53(3):1009–1019, 2005.

[33] Hoang Tuy, *Convex analysis and global optimization*, Springer, 1998.

[34] H L Van Trees. *Detection, estimation, and modulation theory, optimum array processing*. John Wiley & Sons, 2004.

[35] X. Wang, E. Aboutanios, and M. G. Amin, "Adaptive array thinning for enhanced DOA estimation, "*IEEE Signal Processing Letters*, 22:799–803, 2015.

[36] X. Wang, E. Aboutanios, and M. G. Amin, "Slow radar target detection in heterogeneous clutter using thinned space-time adaptive processing," *IET Radar, Sonar & Navigation*, 10(4):726–734, 2016.

[37] X. Wang, M. G. Amin, X. Wang, and X. Cao, "Sparse array quiescent beamformer design combining adaptive and deterministic constraints," *IEEE Transactions on Antennas and Propagation*, 65(11):5808–5818, 2017.

[38] X. Wang, M. Amin, and X. Cao, "Analysis and design of optimum sparse array configurations for adaptive beamforming\, "*IEEE Transactions on Signal Processing*, 66(2) 340–351, 2017.

[39] B Widrow, P E Mantey, L J Griffiths, and B B Goode. Adaptive antenna systems. *Proceedings of the IEEE*, 55(12):2143–2159, 1967.

REPORT DOCUMENTATION PAGE

Form Approved
OMB No. 0704-0188

1. REPORT DATE *(DD-MM-YYYY)*	2. REPORT TYPE	3. DATES COVERED *(From - To)*
07/19/2018	Final	04/01/2017 - 06/30/2018

4. TITLE AND SUBTITLE
Co-Prime Frequency and Aperture Design for HF Surveillance, Wideband Radar Imaging, and Nonstationary Array Processing

5a. CONTRACT NUMBER

5b. GRANT NUMBER
N00014-17-1-2396

5c. PROGRAM ELEMENT NUMBER

6. AUTHOR(S)
Amin, Moeness, G.

5d. PROJECT NUMBER

5e. TASK NUMBER

5f. WORK UNIT NUMBER

7. PERFORMING ORGANIZATION NAME(S) AND ADDRESS(ES)
Villanova University
800 Lancaster Avenue
Villanova, PA19085

8. PERFORMING ORGANIZATION REPORT NUMBER
527998

9. SPONSORING/MONITORING AGENCY NAME(S) AND ADDRESS(ES)
Office of Naval Research
Code 321
875 North Randolph Street
Arlington, VA 22203-1995

10. SPONSOR/MONITOR'S ACRONYM(S)

11. SPONSOR/MONITOR'S REPORT NUMBER(S)

12. DISTRIBUTION/AVAILABILITY STATEMENT
DISTRIBUTION STATEMENT A. Approved for public release. Distribution is unlimited.

13. SUPPLEMENTARY NOTES

14. ABSTRACT
The research objectives are to develop novel co-prime sampling and array design strategies that achieve high-resolution estimation of spectral power distributions and signal direction-of-arrivals (DOAs), and their applications in various surveillance, radar imaging applications, and array processing. The focus of our studies has been in the following two areas: (i) Hybrid Sparse Array Beamforming Design for General Rank Signal Models Generalized co-prime array design; (ii) Optimum Sparse Subarray Design for Multitask Receivers.

15. SUBJECT TERMS
Array signal processing, spectrum estimation, co-prime array, direction-of-arrival estimation, radar imaging, sparse arrays, shared aperture

16. SECURITY CLASSIFICATION OF:			17. LIMITATION OF ABSTRACT	18. NUMBER OF PAGES	19a. NAME OF RESPONSIBLE PERSON
a. REPORT	b. ABSTRACT	c. THIS PAGE			19b. TELEPHONE NUMBER *(Include area code)*
UU	UU	UU	UU	53	

Standard Form 298 (Rev. 8/98)
Prescribed by ANSI Std. Z39.18